DEVELOPMENT OF CONTINUOUS FLOW SYSTEMS FOR CHEMICAL OXYGEN DEMAND DETERMINATION OF WASTEWATER SAMPLES

SUNISA THAPSEANG

A Thesis Submitted to the Graduate School of Naresuan University
in Partial Fulfillment of the Requirements
for the Master of Science Degree in Chemistry
April 2015

Thesis entitled "Development of Continuous Flow Systems for Chemical Oxygen Demand Determination of Wastewater Samples"

By Miss Sunisa Thapseang

has been approved by the Graduate School as partial fulfillment of the requirements for the Master of Science Degree in Chemistry of Naresuan University

Oral Defense Committee

..... Chair

(Kritsana Jitmanee, Ph.D.)

..... Advisor

(Assistant Professor Orawan Kritsunankul, Ph.D.)

..... Co – Advisor

(Associate Professor Jaroon Jakmunee, Ph.D.)

..... Co – Advisor

(Chanyud Kritsunankul, Ph.D.)

..... Internal Examiner

(Assistant Professor Jintana Klamtet, Ph.D.)

Approved

.....

(Panu Putthawong, Ph.D.)

Associate Dean for Administration and Planning

for Dean of the Graduate School

28 APR 2015

ACKNOWLEDGEMENT

The author would like to express her most sincere thanks and appreciation to her supervisor, Assistant Professor Dr. Orawan Kritsunankul, for her supervision guidance, continuous encouragement, assistance and valuable discussion throughout the course of this work and her co-supervisor, Associate Professor Dr. Jaroon Jakmunee (Department of Chemistry, Faculty of Science, Chiang Mai University), for his supervision, valuable discussion and suggestion. The author wishes to thank another thesis co-advisor, Dr. Chanyud Kritsunankul, (Department of Natural Resources and Environment, Faculty of Agriculture Natural Resources and Environment, Naresuan University), for his the suggestion, valuable discussion, continual encouragement and assistance during this research.

The author would like to thank Dr. Kritsana Jitmanee (Department of Chemistry, Faculty of Science, Chiang Mai University) and Assistant Professor Dr. Jintana Klamtet (Department of Chemistry, Faculty of Science, Naresuan University) for being the committee of the thesis examination, comments and discussion. Thanks are also due to Mr. Apichart Boonmalai and Miss Benjaporn Pramote (Ph.D. student, Department of Chemistry, Faculty of Science, Naresuan University) for kindness, offering guidance and discussion.

The author would like to thank Naresuan University and Center of Excellence for Innovation in Chemistry (PERCH-CIC) for partial support.

The author is grateful to thank Department of Chemistry, Faculty of Science, Naresuan University for providing instruments and other research facilities.

The author is very grateful to her family for their tender love, continuous care and encouragement throughout the study. Finally, the author would like to thank those whose names are not here listed and those who have one way or another contributed to the success of this work.

Sunisa Thapseang

Title	DEVELOPMENT OF CONTINUOUS FLOW SYSTEMS FOR CHEMICAL OXYGEN DEMAND DETERMINATION OF WASTEWATER SAMPLES
Author	Sunisa Thapseang
Advisor	Assistant Professor Orawan Kritsunankul, Ph.D.
Co - Advisors	Associate Professor Jaroon Jakmunee, Ph.D. Chanyud Kritsunankul, Ph.D.
Academic Paper	Thesis M.S. in Chemistry, Naresuan University, 2014
Keywords	Chemical oxygen demand, Wastewater, Flow injection analysis, Rapid sequenced aspiration, On-line UV photooxidation, Spectrophotometry

ABSTRACT

A homemade system of a rapid sequenced aspiration of flow analysis (rapid-SAFA) spectrophotometric system with on-line UV photooxidation using two acidified oxidants of potassium dichromate ($K_2Cr_2O_7$) and potassium permanganate ($KMnO_4$) based reactions was constructed and developed for the determination of soluble chemical oxygen demand (COD) of wastewater. This system utilized two techniques of: 1) a rapid sequenced aspiration of standard/sample and reagent solutions into sample loop at UV reactor and 2) a UV photooxidation with acidic $KMnO_4$ and $K_2Cr_2O_7$ solutions to oxidize or digest organic compounds instead of a conventional closed reflux digestion (used in the standard method). A potassium hydrogen phthalate (KHP) was used as COD standard solution throughout this work. For acidified $K_2Cr_2O_7$ based reaction, a potassium peroxydisulfate ($K_2S_2O_8$) was used to accelerate the oxidation reaction of organic compound and an increase in color intensity of chromium(III) ion was spectrophotometrically monitored at 600 nm. For acidified $KMnO_4$ based reaction, a decrease in color intensity of $KMnO_4$ without the use of $K_2S_2O_8$ was spectrophotometrically monitored at 525 nm. The main parameters affecting the system such as reagent concentration of $K_2Cr_2O_7$, $KMnO_4$, $K_2S_2O_8$ and acid solutions, stopped

time at UV reactor, carrier solution, flow rate of carrier, standard/sample and reagent volumes and reaction loop length were studied and optimized.

Under optimum conditions using an acidified $K_2Cr_2O_7$, two linear calibration graphs in the range of 29 - 176 and 176 - 353 mg COD L^{-1} were obtained, with limit of detection values of 27 and 138 mg COD L^{-1}, respectively. A sample throughput was 11.7 injections per hour. Percentages of recovery and relative standard deviation for the analysis of wastewater samples were in the range of 74 - 131 and 0.3 - 10.3, respectively. For using an acidified $KMnO_4$, a linear calibration graph was in the range of 4 - 18 mg COD L^{-1} with a limit of detection of 2.8 mg COD L^{-1}. A sample throughput was 7.5 injections per hour. Percentages of recovery and relative standard deviation for the analysis of wastewater samples were 70 - 128 and 0.2 - 7.9, respectively. The soluble COD values of the proposed system using two acidified oxidants based reaction and UV photooxidation were in good agreement with those obtained from the standard titration method (t-test, 95% confidence level). This system offered several advantages, e.g., low sample and reagent consumption, low waste generation, semi-automatic system, cost effective instrument, easy operation, acceptable accuracy and precision. Especially, the use of UV irradiation for digestion process provides clean, fast and low power option.

LIST OF CONTENTS

Chapter		Page
I	**INTRODUCTION**	1
	Rational for the study	1
	Objectives of the study	2
	Scopes of the study	3
	Expected benefits	3
II	**REVIEW OF RELATED LITERATURE AND RESEARCH**	4
	Wastewater	4
	Chemical oxygen demand	5
	Methods of the determination of COD and literature reviews	7
	Continuous flow analysis	10
III	**RESEARCH METHODOLOGY**	17
	Chemicals	17
	Preparation of solutions	17
	Related reactions	18
	Study of absorption spectra	19
	Design, instrumental setup and procedure of rapid-SAFA spectrophotometric systems	20
	Determination of COD by the rapid-SAFA spectrophotometric system with on-line UV photooxidation	23
IV	**RESULTS AND DISCUSSION**	25
	Study of absorption spectra	25
	Design of the rapid-SAFA systems	25
	Determination of COD by the rapid-SAFA spectrophotometric system with on-line UV photooxidation	26

LIST OF CONTENTS (CONT.)

Chapter		Page
V	CONCLUSIONS	71
	REFERENCES	73
	APPENDIX	80
	BIOGRAPHY	86

LIST OF TABLES

Table		Page
1	Typical concentration of the standard COD values of various water and wastewater sources, assigned by Thepollution Control Department, Ministry of Natural Resources and Environment, Thailand.....	6
2	Continuous flow methods with various on-line sample preparation and detection techniques for the COD determination of water and wastewater samples	8
3	Conditions used of UV-visible spectrophotometer.....	20
4	Preliminary conditions used of the rapid-SAFA spectrophotometric system using acidic $K_2Cr_2O_7$ reagent solution.....	27
5	Effect of standard/sample (V_S) and reagent (V_R) volumes by mean of aspiration times (in second) on peak height of standard KHP solutions (equivalent to COD concentrations).....	28
6	Effect of stopped time at UV reactor on peak height of standard KHP solutions (equivalent to COD concentrations).....	30
7	Effect of $K_2Cr_2O_7$ concentration on peak height and slope of standard KHP solutions (equivalent to COD concentrations).....	32
8	Effect of H_2SO_4 concentration on peak height and slope of standard KHP solutions (equivalent to COD concentrations).....	34
9	Effect of $K_2S_2O_8$ concentration on peak height and slope of standard KHP solutions (equivalent to COD concentrations).....	35
10	Effect of carrier solution using H_2SO_4 on peak height and slope of standard KHP solutions (equivalent to COD concentrations).....	37
11	Effect of reaction loop length at UV reactor on peak height and slope of standard KHP solutions (equivalent to COD concentrations).....	39
12	Effect of flow rate on peak height and slope of standard KHP solutions (equivalent to COD concentrations).....	41

LIST OF TABLES (CONT.)

Table		Page
13	Peak height results of digestion efficiency of some model organic compounds by the rapid-SAFA system using acidic $K_2Cr_2O_7$ reagent solution.....	43
14	Analytical characteristic data of some model organic compounds from the study from the study of digestion efficiency.....	43
15	COD contents and recoveries of some model organic compounds by the rapid-SAFA system.....	45
16	Digestion efficiency by on-line UV photooxidation and conventional digestion on peak height of some model organic compounds.....	46
17	Effect of interference on peak height of 292 mg COD L^{-1} (equivalent to 250 mg L^{-1} KHP); mean of triplicate injections.....	47
18	Conditions used of the system using acidic $K_2Cr_2O_7$ reagent solution.....	47
19	Calibration data of the system for COD determination using acidic $K_2Cr_2O_7$ reagent solution.....	49
20	Preliminary conditions used of the rapid-SAFA spectrophotometric system using acidic $KMnO_4$ reagent solution.....	50
21	Stability study of acidic $KMnO_4$ reagent solution on peak height of standard KHP solution (equivalent to 4 mg COD L^{-1}).....	52
22	Effect of $KMnO_4$ concentration on peak height and slope of standard KHP solutions (equivalent to COD concentration).....	53
23	Effect of H_2SO_4 concentration on peak height and slope of standard KHP solutions (equivalent to COD concentration).....	54
24	Effect of flow rate on peak height and slope of standard KHP solutions (equivalent to COD concentration).....	56
25	Effect of reaction loop length at UV reactor on peak height and slope of standard KHP solutions (equivalent to COD concentration).....	57

LIST OF TABLES (CONT.)

Table **Page**

26 Effect of carrier solution of H_2SO_4 on peak height and slope of standard KHP solutions (equivalent to COD concentration)..... 59

27 Effect of standard/sample (V_S) and reagent (V_R) volumes by mean of aspiration times (in second) on peak height and slope of standards KHP solutions (equivalent to COD concentration)..... 61

28 Conditions used of the system for COD determination using acidic $KMnO_4$ reagent solution..... 62

29 Calibration data of the system for COD determination using acidic $KMnO_4$ reagent solution..... 63

30 Soluble COD contents (mg L^{-1}) in wastewater sample, as determined by the proposed rapid-SAFA spectrophotometric system using acidified $K_2Cr_2O_7$ and $KMnO_4$ based reaction and the standard titration method 66

LIST OF FIGURES

Figure		Page
1	The constituents of wastewater or sewage.....	5
2	(a) The simplest single-line FIA manifold and (b) The analog output has the form of a peak, the recording stating at S (time of injection to), H – peak height, W – peak width at a selected level, A – peak area, T – residence time corresponding to the peak height measurement, and t_b – the peak width at the baseline.....	11
3	Dispersion (D) in the FIA system defined as the ratio between the original concentration (C^0) and the concentration of dispersed specie (C^{max}).....	11
4	General FIA systems, showing its essential components of propelling unit (peristaltic pump), injection, reaction/mixing/modification and detector.....	13
5	Schematic diagram of a basic sequential injection system: P – pump, R – reagent, HC – holding coil, and W – waste.....	14
6	(a) The flow reversal: (i and ii) sequential stacking of sample and reagent in holding coil and (iii) merging of zones on flow reversal to give a zone of product. Arrows show direction of flow, and (b) Structure of injected zones and concentration profiles as seen by the detector; R – reagent, S – sample; P – composite region where the analyte is transformed into a detectable product.....	14
7	Typical schematic diagram of the multicommutated flow injection system (MCFIA) for determination of glucose in honey. P – peristaltic pump; V1, V2, V3 and V4 – 3-way solenoid valves; C – column; TB thermostatic bath; R – reaction coil; D – spectrophotometric detector; and W – waste.....	15

LIST OF FIGURES (CONT.)

Figure		Page
8	Three designs of the rapid-SAFA spectrophotometric system with on-line UV photooxidation for COD determination of: (a) system 1, (b) system 2 and (c) system 3 (C – carrier; R – reagent solution; S – sample/ standard solution; L_{SR} – sample and reagent loop; RC – reaction coil, WC_1 and WC_2 – waste coil 1 and 2 and W_1 and W_2 – waste 1 and 2	21
9	Absorption spectra of: (a) standard KHP solutions (40, 80 and 120 mg L^{-1}) in acidic $K_2Cr_2O_7$ reagent solution (R_1: 0.003 mol L^{-1} $K_2Cr_2O_7$ plus 8.6 mol L^{-1} H_2SO_4) and (b) standard KHP solutions (3, 6 and 9 mg L^{-1}) in acidic $KMnO_4$ reagent solution (R_2: 0.4 mmol L^{-1} $KMnO_4$ plus 0.2 mol L^{-1} H_2SO_4) and a 1×10^{-3} mol L^{-1} $KMnO_4$ solution (R)	26
10	Rapid-SAFA signals for COD determination using three designs of: (a) system 1 and 2 and (b) system 3	26
11	Effect of sample (V_S) and reagent (V_R) volumes by mean of aspiration times (in second) on peak height of standard KHP solutions (300 and 500 mg L^{-1} of KHP equivalent to 335 and 558 mg COD L^{-1})	29
12	Effect of stopped time at UV reactor on peak height of standard KHP solutions (300 and 500 mg L^{-1} of KHP equivalent to 335 and 558 mg COD L^{-1})	31
13	Effect of $K_2Cr_2O_7$ concentration on slope of standard KHP solutions (100 - 300 mg L^{-1} of KHP equivalent to 112 - 353 mg COD L^{-1})	33
14	Effect of H_2SO_4 concentration on slope of standard KHP solutions (100 - 300 mg L^{-1} of KHP equivalent to 112 - 353 mg COD L^{-1})	35
15	Effect of $K_2S_2O_8$ concentration on slope of standard KHP solutions (150 - 300 mg L^{-1} of KHP equivalent to 168 - 353 mg COD L^{-1})	36

LIST OF FIGURES (CONT.)

Figure		Page
16	Effect of carrier solution using H_2SO_4 on slope of standard KHP solutions (150 - 300 mg L^{-1} of KHP equivalent to 168 - 353 mg COD L^{-1})	38
17	Effect of reaction loop length at UV reactor on slope of standard KHP solutions (150 - 300 mg L^{-1} of KHP equivalent to 168 - 353 mg COD L^{-1}), when AT is analysis time.....	40
18	Effect of flow rate on slope of standard KHP solutions (150 - 300 mg L^{-1} of KHP equivalent to 168 - 353 mg COD L^{-1}), when AT is analysis time.....	42
19	Effect of digestion efficiency on: (a) peak heights (250 mg COD L^{-1}, n = 3) and (b) calibration graphs of some model organic compounds by the rapid-SAFA system using acidic $K_2Cr_2O_7$ reagent solution.....	44
20	(a) Typical of a rapid-SAFA signals and (b) calibration graph for COD determination using acidic $K_2Cr_2O_7$ reagent solution.....	50
21	Stability study of acidic $KMnO_4$ reagent solution (0.2 mmol L^{-1} $KMnO_4$ in 0.2 mol L^{-1} H_2SO_4) at 25±2 °C and 12±2 °C by the rapid-SAFA system.....	52
22	Effect of $KMnO_4$ concentration on peak height of standard KHP solutions (10 - 50 mg L^{-1} of KHP equivalent to 12 - 59 mg COD L^{-1}).....	54
23	Effect of H_2SO_4 concentration on peak height of standard KHP solutions (5 - 15 mg L^{-1} of KHP equivalent to 6 - 8 mg COD L^{-1}).....	55
24	Effect of flow rates on slope of standard KHP solutions (5 - 15 mg L^{-1} of KHP equivalent to 6 - 18 mg COD L^{-1}), when AT is analysis time.....	57
25	Effect of reaction loop length at UV reactor on slope of standard KHP solutions (5 - 15 mg L^{-1} of KHP equivalent to 6 - 18 mg COD L^{-1}), when AT is analysis time.....	58

LIST OF FIGURES (CONT.)

Figure **Page**

26 Effect of carrier solution using H_2SO_4 on slope of standard KHP solutions (5 - 15 mg L^{-1} of KHP equivalent to 6 - 18 mg COD L^{-1})..... 60

27 Effect of sample (V_S) and reagent (V_R) volumes by mean of aspiration time (in second) on slope of standard KHP solutions (5- 15 mg L^{-1} of KHP equivalent to 6 - 18 mg COD L^{-1})..... 61

28 (a) Typical of a rapid-SAFA signals and (b) calibration graph for COD determination using an acidic $KMnO_4$ reagent solution..... 64

29 Typical of a rapid-SAFA signals for COD determination using: (a) acidic $K_2Cr_2O_7$ and (b) acidic $KMnO_4$ reagent solutions..... 69

30 Correlation plots between the COD contents of real wastewater samples by: (a) a rapid-SAFA using acidic $K_2Cr_2O_7$ reagent solution and the standard titration method, (b) a rapid-SAFA using acidic $KMnO_4$ reagent solution and the standard titration method and (c) a rapid-SAFA using acidic $K_2Cr_2O_7$ reagent solution and a rapid-SAFA using acidic $KMnO_4$ reagent solution..... 70

31 Setup of a homemade rapid-SAFA spectrophotometric system, designed and constructed by Chanyud Kritsunankul, Orawan Kritsunankul and Jaroon Jakmunee..... 81

32 Setup of a standard titration method..... 82

ABBREVIATIONS

$\overline{x}$	=	Arithmetic mean, Average
FIA	=	Flow injection analysis
g	=	Gram
i.d.	=	Inner diameter
LOD	=	Limit of detection
mg L^{-1}	=	Milligram per liter
mL	=	Milliliter
mL min^{-1}	=	Milliliter per minute
MW	=	Molecular weight
mol L^{-1}	=	Mole per liter
nm	=	Nanometer
No.	=	Number
RSD	=	Relative standard deviation
% Rec	=	Percentage recovery
% w/v	=	Percentage weight by volume
PTFE	=	Polytetrafluoroethylene
Rapid-SAFA	=	Rapid sequenced aspiration flow analysis
s	=	Second
r^2	=	Square of correlation coefficient
SD	=	Standard deviation
UV	=	Ultraviolet

CHAPTER I

INTRODUCTION

Rational for the study

In general, **water and wastewater quality indicators** are tested in laboratory to assess suitability of water and wastewater for use or re-use or disposal [1, 2]. Those tests can be divided into three characteristics of water; physical, biological, and chemical [3]. Physical characteristics are designed to measure various group of constituents directly impact water and wastewater treatability such as total solids, total dissolved solids, total suspended solids, turbidity, salinity, pH value, temperature, odor, color, and taste. Biological characteristics are aimed to measure the approximate biological population of water and wastewater, such as *Escherichia coli* (E.coli), coliform bacteria and other disease-causing bacteria. For chemical characteristics, they are proposed to determine the concentration of targeted chemical species that may be found in water and wastewater, for example 1) heavy metals (e.g., antimony, arsenic, cadmium, copper, chromium, iron, lead and zinc) that may be essential to plant growth while others adversely affect water consumers, wastewater treatment systems, and receiving waters, 2) nutrients (e.g., nitrogen and phosphorus species) that can contribute to the acceleration of eutrophication and 3) organic matters (e.g., biochemical oxygen demand (BOD), chemical oxygen demand (COD), total organic carbon (TOC), and oil and grease (O&G)) that are a measurement of the relative oxygen-depletion effect and/or a carbon-based compound measurement of a water and wastewater contaminant.

In the part of **organic matter** in water and wastewater that cause problems with oxygen depletion in streams, because as microbes metabolize organic material, they consume oxygen, it is a matter composed of organic compounds that can come from various situations of water sources, for example 1) seawater ingress, 2) direct ingress of river water, 3) infiltrated groundwater into sewage, 4) drainage or rainfall runoff from industrial, highway, road, hospital, urban, or agriculture, 5) human waste, 6) industrial waste, 7) sewage treatment plant and septic tank discharges, and 8) cesspit leakage [1, 2]. Therefore, a quantity of organic matters or compounds is very important parameter

to indicate or assess quality of water and wastewater. Consequently, in this work, the main focus of the organic matter test for wastewater quality indicator is COD which is simple, rapid and less analysis time than BOD test and less experimental equipments than TOC test.

Several analytical techniques have been used and applied for COD determination in water and wastewater with good accuracy and precision. These techniques include titration [4, 5, 6, 7, 8, 9] and ultraviolet-visible spectrophotometry [4, 10, 11, 12] as standard methods, chemiluminescence [13, 14], fluorescence [15] and electrochemistry [16, 17, 18]. According to reviewed papers, titration and ultraviolet-visible (UV-visible) spectrophotometric methods are commonly used for determination of COD in water and wastewater using several sample digestion techniques such as closed reflux or opened reflux, ultrasonic, water bath and microwave. Some of these digestion techniques have several drawbacks such as non-automated technique, tedious in operation, high consumption of reagent and sample solution, high waste generation and long analysis time. To compromise of these reasons for COD determination, the continuous flow system such as flow injection analysis (FIA) [19, 20, 21, 22, 23, 24, 25, 26, 27, 28, 29, 30] and sequential injection analysis (SIA) [31, 32] are required to determine COD content. Moreover, a rapid sequenced flow injection system [33, 34] or a multicommutated flow injection system [35, 36], the additional of continuous flow injection techniques is also interested for the proposed reason.

In this present work, a homemade system of a rapid sequenced aspiration flow analysis (rapid-SAFA) spectrophotometry was constructed and developed for the determination of soluble COD in wastewater. This system utilized two acidified oxidants of potassium dichromate ($K_2Cr_2O_7$) and potassium permanganate ($KMnO_4$) based reactions coupled with an on-line UV photooxidation to oxidize or digest organic compounds in wastewater. The proposed system gained semi-automatic feature, easy operation, low sample and chemical consumption, low waste generation, cost-effective instrument and acceptable accuracy and precision.

Objectives of the study

1. To construct and develop a homemade rapid-SAFA spectrophotometric system with an on-line UV photooxidation for the determination of soluble COD.

2. To optimize the proposed system using an acidic $K_2Cr_2O_7$ reagent solution and apply for soluble COD determination of wastewater samples.

3. To optimize the proposed system using an acidic $KMnO_4$ reagent solution and apply for soluble COD determination of wastewater samples.

Scopes of the study

Contents of soluble COD of wastewater samples will be determined by the developed of a homemade rapid-SAFA spectrophotometric system with on-line UV photooxidation. This system is optimized for oxidation or digestion of organic compounds in wastewater using two acidic reagent solutions of $K_2Cr_2O_7$ and $KMnO_4$ with UV irradiation. The proposed systems should offer several advantages, e.g., less reagent and sample consumptions, acceptable analysis time, low waste generation, semi-automatic system, easy operation and acceptable accuracy and precision.

Expected benefits

1. Achieve the homemade rapid-SAFA spectrophotometric system with on-line UV photooxidation for soluble COD determination of wastewater samples.

2. Present the research work in the national and/or international academic conference by poster and/or oral presentation or published the academic paper.

CHAPTER II

REVIEW OF RELATED LITERATURE AND RESEARCH

Wastewater

Wastewater is water containing everything from a community, including household waste, commercial and industrial waste, stream flow, and storm water and groundwater without treatment [3]. All effluent wastewaters may change the water quality, environmental and ecological impact. The constituents of wastewater (or sewage) could be divided into dissolved and suspended solids matters or compounds (Figure 1). Dissolved matters refer to organic and inorganic matter passing through a glass microfiber filters while suspended solid matter refers to organic and inorganic matters retained by glass microfiber filters. Dissolved organic matters commonly relevant to 'soluble COD' or 'dissolved COD' in water that includes primarily of proteins, carbohydrates, long-chain saturated hydrocarbons and other complex compounds and pathogens. As for dissolved inorganic matters in water, they are such as chemical compounds or complexes or ions of chloride, alkalinity, sodium, magnesium, calcium, fluoride and heavy metals. In the part of suspended solid or particulate matters found in wastewater, it includes silt, clay and fine particles of organic and inorganic matters and other microscopic organisms [37, 38, 39]. This suspended organic matters also refer to 'suspended COD' or 'particulate COD'. Consequently, in this research, the main focus of organic matters or compounds in water was soluble COD for estimation of wastewater quality.

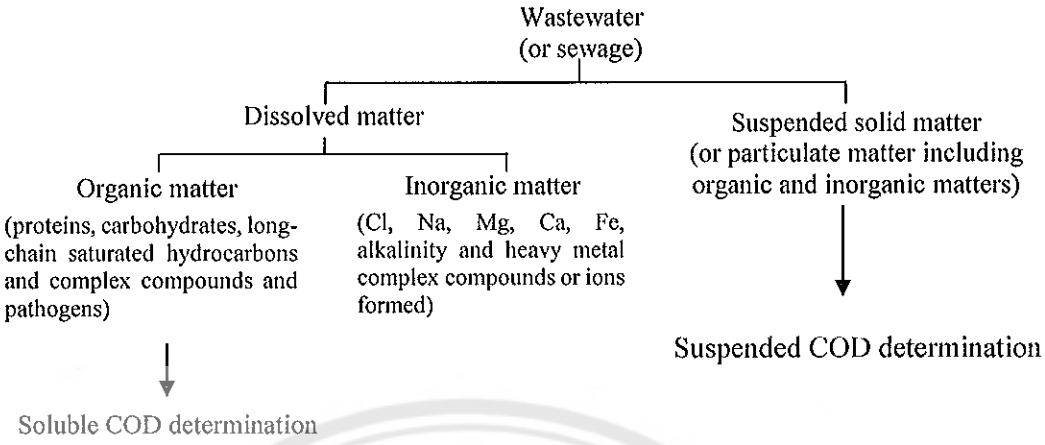

Figure 1 The constituents of wastewater or sewage [37, 38, 39]

Chemical oxygen demand

Chemical oxygen demand (COD), especially in environmental chemistry, commonly used to indirectly measure the amount of organic matters or compounds in water and wastewater [4, 5]. It represents that nearly all organic compounds (CHON) can be fully oxidized to carbon dioxide (CO_2) and water (H_2O), including ammonia (NH_3) or ammonium ion (NH_4^+) as shown in equation (1) [40].

$$C_nH_aO_bN_c\,(aq) + \left(n + \frac{a}{4} - \frac{b}{2} - \frac{3c}{4}\right) O_2\,(g) \rightarrow nCO_2\,(g) + \left(\frac{a}{2} - \frac{3c}{2}\right) H_2O\,(l) + cNH_3\,(g) \quad \text{.....(1)}$$

The condition of COD test usually uses strong oxidizing agent (e.g., $KMnO_4$ and $K_2Cr_2O_7$) to oxidize organic compounds under acidic conditions, usually achieved by the addition of sulfuric acid (H_2SO_4). For $K_2Cr_2O_7$ as an oxidizing agent, the reaction of $K_2Cr_2O_7$ with organic compound is given by following common equation (2) [40, 41].

$$C_nH_aO_bN_c\,(aq) + dCr_2O_7^{2-}\,(aq) + (8d+C)\,H^+\,(aq) \xrightarrow[\text{Heat}]{\text{Catalyst}} nCO_2\,(g) + \frac{a+8d-3c}{2} H_2O\,(l) + cNH_4^+\,(g) + 2dCr^{3+}\,(aq) \quad \text{.....(2)}$$

The consumed oxidant was calculated and expressed in terms of oxygen equivalence which indicates the milligram of oxygen consumed per litter (mg O_2 L^{-1}) of solution that so call COD value or milligram of COD per litter (mg COD L^{-1}). This COD test using $K_2Cr_2O_7$ is non-specific, in that it does not identify the oxidizable compounds or differentiate between the organic and inorganic compound. Similarly, it does not indicate the total organic carbon species since some organic compounds are not oxidized by $K_2Cr_2O_7$ whereas some inorganic compounds are oxidized. Nevertheless, COD is a useful, rapidly measured, variable for many wastewater sources and has been used for several decades [3]. Therefore, the COD concentrations could be used to observe the quality of various water and wastewater sources, for example: in the range of 20 mg O_2 L^{-1} in surface waters (or unpolluted water) to greater than 200 mg O_2 L^{-1} in waters receiving effluents, 100 to 60000 mg O_2 L^{-1} in industrial wastes [38] and 250 to 1000 mg O_2 L^{-1} in untreated domestic wastewater [1]. Moreover, in Thailand, the standard COD values are also assigned and assessed to control water and wastewater quality by the Pollution Control Department (PCD), Ministry of Natural Resources and Environment [42]. These values are shown in Table 1.

Table 1 Typical concentration of the standard COD values of various water and wastewater sources, assigned by The Pollution Control Department, Ministry of Natural Resources and Environment, Thailand [42]

Water and wastewater source	COD (mg O_2 L^{-1})
Industrial factory	< 400
Pig farm	< 400
Irrigation system	< 100
Gas station and oil terminal	< 200
Untreated domestic wastewater	Low (< 250) medium (< 500) high (< 1000)

Methods of the determination of COD and literature reviews

Many analytical methods have been published for COD determination of water and wastewater with good accuracy and precision. These methods include titration and UV-visible spectrophotometry, chemiluminescence, fluorescence and electrochemistry.

Methods of titration [5, 6, 7, 8, 9] and UV-visible spectrophotometry [10, 11, 12] were commonly used to determine COD and have been established as standard reference methods of water and wastewater treatment [4]. These methods are based on the oxidation and digestion of potassium hydrogen phthalate (KHP) as standard solution with acidic $K_2Cr_2O_7$ under conditions of high temperature (150 °C) and long digestion time (2 hours). After that, for titration, an excess $K_2Cr_2O_7$ was titrated with ferrous ammonium sulfate utilizing 1, 10-phenanthroline ferrous sulfate as indicator and then the COD value was obtained by calculation. Meanwhile, spectrophotometric method was monitored chromium(III) ion at 600 nm and the COD value was obtained by the standard calibration method.

For chemiluminescence methods, a standard or sample were firstly oxidized with acidic $K_2Cr_2O_7$ [13] or acidic $KMnO_4$ [14] and digested by closed reflux. Soon after that, the production of Cr(III) and Mn(II) were reacted with chemiluminescence solution such as luminol-H_2O_2 [13] and glutaraldehyde [14] solutions to produce luminol-H_2O_2-Cr(III) and glutaraldehyde-Mn(II) complex compounds and then they were monitored by photodiode and photomultiplier tube, respectively. From the analysis, the light intensity of Cr(III) or Mn(II) concentrations was proportional to COD value of sample. Moreover, fluorescence method [15] was also applied for COD determination using acidic cerium sulphate ($(Ce(SO_4)_2)$) and UV lamp for oxidation and degradation of standard or sample. Then, the Ce(III) was monitored at 264.8 nm of excitation and 362.1 nm of emission wavelengths. The light intensity of Ce(III) concentrations was proportional to COD value in sample.

And other method of electrochemistry by polarography [17] was reported for COD determination using the combination of digestion technique. It was based on the oxidation and digestion of KHP with reagent solution ($K_2Cr_2O_7$+H_2SO_4+H_3PO_4) and opened reflux. The excess Cr(VI) was measured by single sweep polarography. The COD content can be indirectly calculated by measuring the Cr(VI) consumed.

In addition, the continuous flow methods using widely different on-line sample preparation and detection techniques have been published for COD determination in water and wastewater. These continuous flow methods are summarized in Table 2.

Table 2 Continuous flow methods with various on-line sample preparation and detection techniques for the COD determination of water and wastewater samples

Techniques	Details*	Year [Ref.]
1. FIA / water bath / UV-visible spectrophotometry	• Samples: civic, dye and wool-spinning wastewaters • Conditions: using reagent solution of 5×10^{-3} mol L^{-1} $KMnO_4$ + 6% H_2SO_4 + 0.1 mol L^{-1} $(NH_4)_2SO_4$, on-line digestion at 95 °C for 8 min and detection at 525 nm • Analytical characteristics: LR = 10-80 mg COD L^{-1}, LOD = 2 mg COD L^{-1}, SP = 80 h^{-1}, RSD = 0.7 %, recoveries = 85-95 %	1992 [19]
2. FIA / microwave digestion / UV-visible spectrophotometry	• Samples: well, river and muzza canal waters and sewage and food industry wastewaters • Conditions: using reagent solution of 0.4 mol L^{-1} $K_2Cr_2O_7$ + 18.38 mol L^{-1} H_2SO_4, on-line digestion at 180 W for 3 min and detection at 445 nm • Analytical characteristics: LR = 0-100 mg COD L^{-1}, LOD = 1.5 mg COD L^{-1}, RSD < 4.5 %	1992 [20]
3. FIA / microwave digestion / flame atomic absorption spectrometry	• Samples: urban and industrial wastewaters • Conditions: using reagent solution of 0.0167 mol L^{-1} $K_2Cr_2O_7$ + 3 mol L^{-1} H_2SO_4, on-line digestion at 662 W for 15 min and detection at 428.6 nm • Analytical characteristics: LR = 25-5000 mg COD L^{-1}, LOD = 7 mg COD L^{-1}, SP > 50 h^{-1}, RSD < 8.6 %	1996 [21]
4. FIA / water bath / UV-visible spectrophotometry	• Samples: natural waters • Conditions: using reagent solution of 8×10^{-4} mol L^{-1} $KMnO_4$ + 0.6 mol L^{-1} H_2SO_4, on-line digestion at 50 and 80 °C and detection at 525 nm • Analytical characteristics: LR = 0.1-5.9 mg COD L^{-1}, LOD = 80 µg COD L^{-1}, SP = 18 h^{-1}, RSD =1.3-4.8 %	1999 [22]

Table 2 (cont.)

Techniques	Details	Year [Ref.]
5. FIA / UV-photocatalytic oxidation / UV-visible spectrophotometry	• Sample: Tamar river waters • Conditions: using reagent solution of 8×10^{-4} mol L^{-1} $KMnO_4$ + 0.3 mol L^{-1} H_2SO_4, on-line digestion at 15 W UV lamp for 1.5 min and detection at 524 nm • Analytical characteristics: LR = 0.5-50 mg COD L^{-1}, LOD = 0.5 mg COD L^{-1}, SP = 30 h^{-1}, RSD = 1.21-2.7 %, recoveries = 83-111 %.	2005 [25]
6. FIA / water bath/ UV-visible spectrophotometry	• Sample: river waters • Conditions: using reagent solution of 0.2 mmol L^{-1} $KMnO_4$ + 1 mmol L^{-1} HIO_4 + 0.8 mol L^{-1} H_2SO_4, on-line digestion at 70 °C and detection at 525 nm • Analytical characteristics: LR = 1.0-24 mg COD L^{-1}, LOD = 0.5 mg COD L^{-1}, SP = 30 h^{-1}, RSD = 0.4 %	2006 [26]
7. FIA / microwave digestion / inductively coupled plasma optical emission spectrometry	• Sample: domestic sewage, dairy and dye wastewaters and river waters • Conditions: using reagent solution of 0.0167 mol L^{-1} $K_2Cr_2O_7$ + concentrated mol L^{-1} H_2SO_4, on-line digestion at 360 W and detection at 357.9 nm • Analytical characteristics: LR = 2.78-850 mg L^{-1}, LOD = 0.94 mg COD L^{-1}, SP = 18 h^{-1}, RSD = 0.41-0.85 %, recoveries = 96-99 %	2012 [29]
8. FIA / microwave digestion / inductively coupled plasma optical emission spectrometry	• Sample: domestic sewage, dairy and dye wastewaters and river waters • Conditions: using reagent solution of 0.2 g L^{-1} $KMnO_4$ + concentrated H_2SO_4, on-line digestion at 350 W and detection at 294.92 nm • Analytical characteristics: LR = 2.6-850 mg COD L^{-1}, LOD = 1.25 mg COD L^{-1}, SP = 22 h^{-1}, RSD = 0.34 %, recoveries = 96.4-100 %	2012 [30]

*LR – Linear range, LOD – limit of detection, SP – sample throughput

Continuous flow analysis

1. Flow injection analysis

Flow injection analysis (FIA) is a well-known new way of performing wet chemistry that firstly reported by Ruzicka and Hansen in 1975. FIA system is simple, automated microchemical technique, capable of having a high sampling rate and a minimum sample and reagent consumption, which is more efficient than classical method [43, 44, 45]. A simplest diagram of the FIA system is shown in Figure 2 (a). Basically, the FIA system is based on injection of the exact standard or sample volume into a continuous flow of carrier or reagent stream by passing through injection valve within a small diameter tubing. The constant flow rate of carrier or reagent stream was controlled by a pump. The injected sample zone is mixed and dispersed into the reagent zone at reaction or mixing coils to form the product. The product zone are transported toward a detector and then continuously recorded the absorbance, potential, or other physical parameters [46]. A FIA peak occurs due to two processes involve the simultaneous physical process of zone dispersion and the chemical process. A typical recorder output has the form of a peak in Figure 2 (b) [45]. The FIA peak is used to quantify the analyte using calibration data from known concentrations of the standard [47]. FIA system can be also incorporated to several sample preparation and separation methods (such as solvent extraction, dialysis, heating, and other methods) and detection techniques (such as spectrophotometry, electrochemical and other techniques). A FIA systems have been widely applied to determine various samples such as food, mineral material, clinical, water and other samples [46, 47, 48].

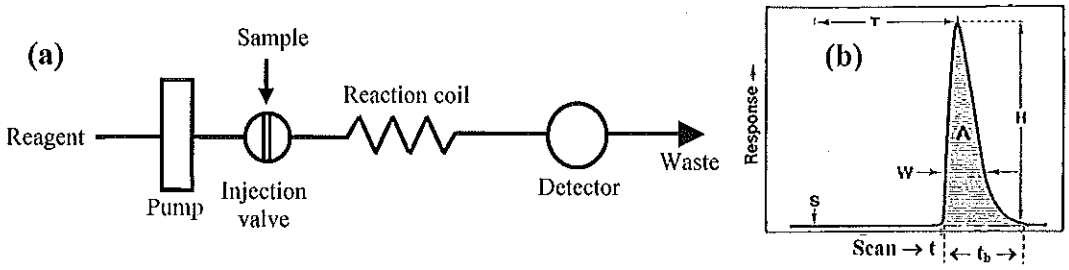

Figure 2 (a) The simplest single-line FIA manifold and (b) The analog output has the form of a peak, the recording stating at S (time of injection), H – peak height, W – peak width at a selected level, A – peak area, T – residence time corresponding to the peak height measurement, and t_b – peak width at the baseline [45, 49]

A ***basic principle of FIA*** depends on a combination of three important principles; 1) sample injection, 2) controlled dispersion of the injection sample zone, and 3) reproducible timing of the movement of injected zone from the injection point to the detector. Especially, ***dispersion*** is the most important parameter and considers when the sample is introduced into a carrier stream and during transport of the zone to the detector [46]. Dispersion (see in Figure 3) could be described in single-line FIA manifold and defined as the amount that the chemical signal is reduced by injecting a sample plug into an FIA system. This is expressed in terms of *dispersion coefficient (D)* which is defined as the ratio of the original concentrations (C^o) of the injection sample and the maximum concentration (C^{max}) of the sample zone ($D = C^o / C^{max}$) after it has undergone all the dispersive processes and is passing through the detector [50, 51, 52].

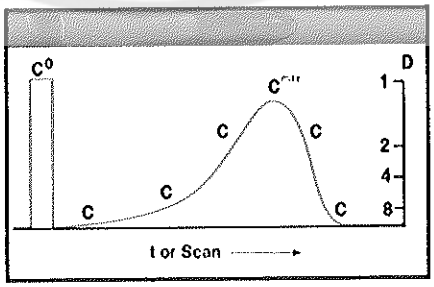

Figure 3 Dispersion (D) in the FIA system defined as the ration between the original concentration (C^0) and the concentration of dispersion species (C^{max}) [43]

The terms of dispersion are categorized into limited, medium and large dispersions. Limited dispersion (D = 1-3) is used in conjunction with detection system such as an ion-selective electrode or an atomic absorption spectrometry, where minimal sample dilution is desirable. Medium dispersion (D = 3-10) is most commonly used where significant sample and reagent mixing is necessary, as is the case for methods involving spectrophotometric or fluorometric detection. Large dispersion (D > 10) is used where extensive dilution of sample and reagent is required [51]. The dispersion is controlled through the suitable choices of sample injection volume, flow rate, and length and diameter of tubing [53]. The volume of injection, which most cases is the sample, is important factor influencing its dispersion. In general when increased dispersion, the chemistry effect causes predominant effect between analyte and reagent by enhance sensitivity, but the dilution effect leads to a lowering sensitivity, increasing peak broadening and reducing sample throughput. Therefore, in developing a new methodology, the analyst must find a set of conditions that gives the best balance between enhancement of chemistry and dilution for the application of interest [52].

The ***basic components*** of a FIA system are consisted of four parts (Figure 4) including propelling, injecting or insertion, transport, and detection or sensing systems. Each of these components is described as follows [54].

1. *A propelling system* which drives the carrier stream to the difference elementary units of the system. Ideally, it should provide a pulse-free and perfectly producible flow of constant rate. A propelling system can be propelled by various types of pump such as peristaltic pump, gas pressure and piston or syringe pump.

2. *An injection* or *insertion system* for introduction of variable sample volumes into the carrier stream in a highly accurate and reproducible manner. Many of injection system are used such as a rotary injection valve and hydrodynamic injection valve.

3. *A transport system* in which the sample zone disperses and reacts with the components of the carrier stream, forming a species which is sensed by a flow through detector and recorded. There are coiled reaction, knotted reactor and digestion or separation device.

4. *A detection* or *sensing system* allowing continuous monitoring of a given property of the sample or its reaction product and providing qualitative and quantitative

information about the former. The most common detectors in FIA are spectrophotometer, photometer, and fluorometer. Electrochemical, chemiluminescence, atomic emission and atomic absorption detectors have also been used.

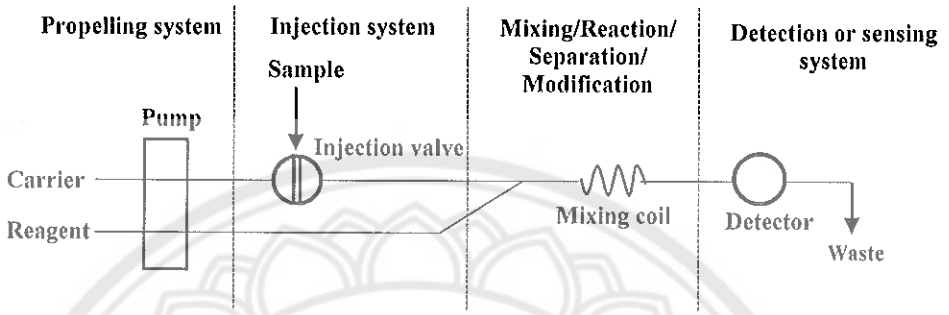

Figure 4 General FIA system, showing its essential components of propelling unit (peristaltic pump), injection, reaction/mixing/modification and detector [51]

2. Sequential injection analysis

Sequential injection analysis (SIA) is the several generation of flow measurement techniques in chemical analysis, and it quickly gains numerous applications in various fields of chemical analysis such as food and environment [48]. The SIA system is sequentially introduced of sample/standard and reagent by multi-position selection valve to stack zones in the tubing that the volume of sample and reagent used are controlled by aspiration time. Furthermore, a SIA system uses a computer control in order to ensure the reproducibility of the flow pattern in process [31]. The schematic diagram of a basic sequential injection manifolds is shown in Figure 5. A SIA manifold are comprised the following main components: pump, holding coil, selection valve, reactor or reaction coil, detector and software. The sample and reagent solutions are sequential aspirated through multi-position selection valve into a holding coil by pump in the reverse mode. In injection step or the forward mode, the pump propels the stacked of sample and reagent zones through a reaction coil into the detector. The flow reversal leads to mixing of the sample and reagent zones to create at a zone of product whose properties are measured at the detector [32, 55]. Figure 6(a) and 6(b) show the overlapped zone of reagent (R) and sample (S) solution and the overlap zone

of peak at detector by sequential injection sample and reagent zone formed to product, respectively. The SIA has several advantages when compared with tradition flow injection. Not only is reagent usage lower with SIA but the manifold used are simple. It is also easy to change from one analytical procedure to another by altering the flow program.

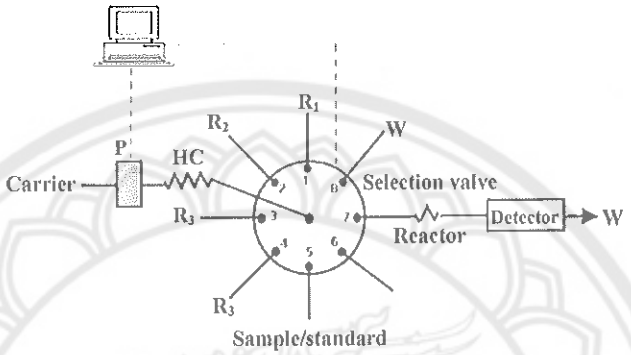

Figure 5 Schematic diagram of a basic sequential injection system : P – pump, R – reagent, HC – holding coil and W -waste [31]

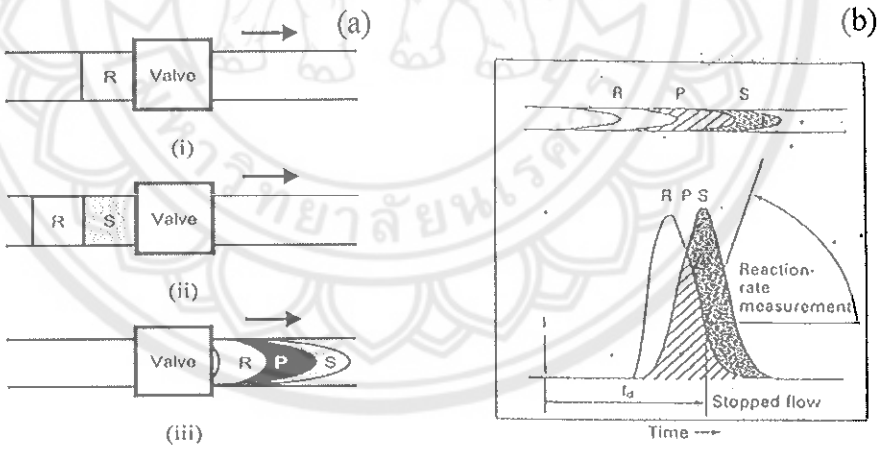

Figure 6 (a) The flow reversal: (i and ii) sequential stacking of sample and reagent in holding coil and (iii) merging of zones on flow reversal to give a zone to give a zone of product. Arrows show direction of flow [32], **and (b) Structure of injected zones and concentration profiles as seen by the detector; R – reagent; S – sample; P – composite region where the analyte is transformed into a detectable product** [48]

3. Multicommutated flow injection analysis

The multicommutated flow injection analysis (MCFIA) is new approach for sample and reagent handing in continuous-flow system. This system require the computer to control the operation of the valves and uses three-way solenoid commutation valves replaced six-port rotary valves in FIA system with introducing flexibility and save solutions [36]. The MCFIA system comprises a multi-channel peristaltic pump and a combination of solenoid commutation valves. The sample and reagent are sequentially introduced of very small segments into the reacting device by operating alternately of solenoid commutation valves that the injected sample volume can be selected by controlling the commutation timing via software. And then, the peristaltic pump propels the liquid or segments of sample and reagent toward detector [56]. The schematic diagram of a typical MCFIA system for glucose determination is shown in Figure 7. The MCFIA analysis presents some advantages such as a high flexibility and a low investment cost since solenoid valves are inexpensive [57]. In addition, this system has been developed to address some drawbacks of FIA, namely high consumption of reagents and the use multi-channel manifolds. Furthermore, MCFIA method have been applied to many applications such as metal, environmental, food and pharmaceutical samples.

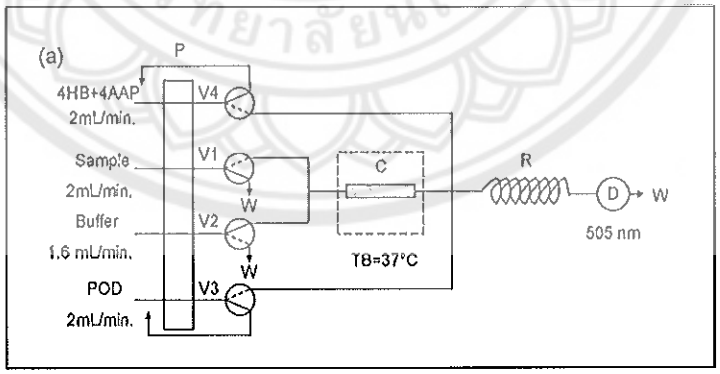

Figure 7 Typical schematic diagram of the multicommutated flow injection system (MCFIA) for determination of glucose in honey. P – peristaltic pump; V1; V1, V2, V3 and V4 – 3-way solenoid valves; C - column; TB – thermostatic bath; R - reaction coil; D – spectrophotometric detector; and W - W - waste [57]

However, the analysis system used in this work was based on the concept of the continuous flow analysis of FIA, SIA and MCFIA and developed for COD determination in wastewater. This system was named a rapid sequenced aspiration of flow analysis (rapid-SAFA) spectrophotometry.

CHAPTER III

RESEARCH METHODOLOGY

Chemicals

All chemicals were analytical reagent grade and were used without further purification. Chemicals are listed as follows:

1. Potassium hydrogen phthalate [$K_8H_5KO_4$]: 99.8%, Ajax finechem, Australia
2. Potassium dichromate [$K_2Cr_2O_7$]: 99.8%, Ajax finechem, Australia
3. Potassium permanganate [$KMnO_4$]: 99%, Ajax finechem, Australia
4. Potassium peroxydisulfate [$K_2S_2O_8$]: 96%, Merck, Germany
5. Sulfuric acid [H_2SO_4]: 96%, LAB-SCAN, Ireland
6. Glucose [$C_6H_{12}O_6$]: > 99%, Ajax finechem, Australia
7. Citric acid [$C_6H_8O_7.H_2O$]: 99.7%, BDH, England
8. Sorbic acid [$C_6H_7KO_2$]: 99%, Fluka, Switzerland
9. Benzoic acid [$C_7H_5NaO_2$]: 99%, Fluka, Switzerland
10. Gallic acid [$C_7H_6O_5.7H_2O$]: 98%, Sigma-Aldrich, USA
11. Sodium nitrite [$NaNO_3$]: 97%, Ajax finechem, Australia
12. Magnesium nitrate [$Mg(NO_3)_2.6H_2O$]: 99%, Loba Chemie, USA
13. Sodium chloride [NaCl]: 99%, LAB-SCAN, Ireland
14. Ferrous ammonium sulfate [$(NH_4)_2Fe(SO_4)_2.6H_2O$]: 99%, Merck, Germany
15. Ferric sulfate [$Fe(SO_4)_3$]: 23 % as Fe, Ajax finechem, Australia

Preparation of solutions

All chemical solutions were prepared in ultrapure water with resistivity 18.2 MΩ.cm (Elgastat maxima, England) throughout this work.

1. Stock standard solution of potassium hydrogen phthalate (1000 mg L^{-1} KHP)

A 0.1002 g of KHP was dissolved in 100 mL water and kept at 4 °C before analysis. This 1000 mg L^{-1} KHP solution has a theoretical COD of 1176 mg COD L^{-1} (calculated in appendix B1 and B2). Working standard solutions of KHP were freshly prepared by dilution of 1000 mg L^{-1} KHP with water.

2. Acidic potassium dichromate reagent solution (0.025 mol L^{-1} $K_2Cr_2O_7$ in 0.5 mol L^{-1} H_2SO_4)

A 2.70 mL of concentrated H_2SO_4 and a 25.0 mL of 0.1 mol L^{-1} $K_2Cr_2O_7$ (containing 2.94 g of $K_2Cr_2O_7$ in 100 mL water) were firstly prepared and then a 3% w/v of $K_2S_2O_8$ was added and dissolved before made up to a final volume of 100 mL volumetric flask with water.

3. Acidic potassium permanganate reagent solution (0.4 mmol L^{-1} $KMnO_4$ in 0.2 mol L^{-1} H_2SO_4)

A 0.0063 g of $KMnO_4$ was dissolved in 50 mL water and then a 1.09 mL of concentrated of H_2SO_4 was added before made up to a final volume of 100 mL volumetric flask with water. This solution was filtered and kept in the dark at 12 ± 2 °C of ice container before analysis.

4. Wastewater

Wastewater samples were collected from various sources (i.e. agricultural drainage, domestic, hospital and pig farm) without acidic preservation, kept at about 4 °C and filtered before analysis. All filtrated samples were analyzed within 24 hours.

Related reactions

The determination of COD in this work is based on redox reaction combined with a UV catalytic irradiation (or a UV photooxidation). The redox reaction is adapted from '*the standard methods for the examination of water and wastewater*' [4] for COD determination using $K_2Cr_2O_7$ and $KMnO_4$ as oxidizing agents. The UV photooxidation reaction is also applied from literature reviews using UV photooxidation reaction for determination of dissolved reactive phosphorus and dissolved inorganic phosphorus in natural water [56] and determination of dissolved organic carbon and dissolved inorganic carbon in water [57].

Under conditions using acidified $K_2Cr_2O_7$ based reaction, the KHP (used as COD standard solution) is oxidized with acidic $K_2Cr_2O_7$ coupled with UV irradiation using $K_2S_2O_8$ as catalytic reagent (shown in equation (3)). The increased in color intensity of chromium(III) ion (Cr^{3+}) was detected by UV-visible spectrophotometry.

$$KC_8H_5O_4\,(aq) + 10K_2Cr_2O_7\,(aq) + 41H_2SO_4\,(aq) \xrightarrow[\text{plus } K_2S_2O_8]{h\nu \text{ UV irradiation (UV lamp of 36 W)}} 16CO_2\,(g) + 46H_2O\,(l) + 10Cr_2(SO_4)_3\,(aq) + 11K_2SO_4\,(aq) \quad \text{.....(3)}$$

For acidified $KMnO_4$ based reaction, the KHP is oxidized with acidic $KMnO_4$ coupled with UV radiation without catalytic reagent (shown in equation (4)). The decrease in color intensity of $KMnO_4$ was detected by UV-visible spectrophotometer.

$$2KC_8H_5O_4\,(aq) + 12KMnO_4\,(aq) + 12H_2SO_4\,(aq) \xrightarrow{h\nu \text{ UV irradiation (UV lamp of 36 W)}} 12MnSO_4\,(aq) + 7K_2SO_4\,(aq) + 24H_2O\,(l) + 16CO_2\,(g) \quad \text{..... (4)}$$

These two reactions for COD determination were preliminary investigated the absorption spectra by UV-visible spectrophotometer and then adopted for further study of a rapid-SAFA system.

Study of absorption spectra

In order to select a suitable maximum wavelength for COD determination using an acidified $K_2Cr_2O_7$ and $KMnO_4$ based reactions. All solutions were prepared as follows. For the usage of acidic $K_2Cr_2O_7$ as reagent solution, KHP solutions (40, 80 and 120 mg L^{-1}) in reagent solution (0.003 mol L^{-1} $K_2Cr_2O_7$ + 8.6 mol L^{-1} H_2SO_4) were prepared and then digested by closed reflux at 150 °C for 2 hours. As for acidic $KMnO_4$ reagent solution, KHP solutions (3, 6 and 9 mg L^{-1}) in reagent solution (0.4 mmol L^{-1}

$KMnO_4$ + 0.2 mol L^{-1} H_2SO_4) were prepared and digested at 100 °C of water bath for 30 min. A higher concentration of 0.001 mol L^{-1} $KMnO_4$ was also prepared. These solutions were recorded all absorption spectra by a UV-visible spectrophotometer (V-650 spectrophotometer, Jasco, Japan) with SpectraManager software for the analysis. Conditions used of UV-visible spectrophotometer is shown in Table 3.

Table 3 Conditions used of UV-visible spectrophotometer

Parameter	Conditions used
Start wavelength	200 nm
End wavelength	900 nm
Scan speed	400 nm min^{-1}
Smooth	2 nm

Design, instrumental setup and procedure of rapid-SAFA spectrophotometric systems

1. Design and instrumental setup

The systems of rapid-SAFA spectrophotometry with on-line UV photooxidation were designed and constructed by research groups of Chanyud Kritsunankul (Department of Natural Resources and Environment, Faculty of Agriculture Natural Resources and Environment, Naresuan University, Phitsanulok, Thailand), Orawan Kritsunankul (Department of Chemistry, Faculty of Science, Naresuan University, Phitsanulok, Thailand) and Jaroon Jakmunee (Department of Chemistry, Faculty of Science, Chiang Mai University, Chiang Mai, Thailand). All designed systems are shown in Figure 8. These systems were different in the position of UV reactor and peristaltic pumps. Each of systems consisted of peristaltic pumps (P_1 and P_2; Masterflex, Cole-parmer, USA), three-way solenoid valves (SV_1, SV_4 and SV_5; Cole-parmer, USA), two-way solenoid valves (SV_2 and SV_3; Cole-parmer, USA), a homemade UV reactor (36 W of UV lamp wound with PTFE tubing (i.d. 0.89 mm), a homemade degassed unit (DU; consisted of two acrylic sheets and PTFE membrane), a flow through cell (FC; 10 mm path length, Perkin elmer, USA), a UV-visible

spectrophotometer (D; Spectro SC, Labomed, U.S.A), a homemade controller (made by Chanyud Kritsunankul) and a homemade interface (made by Jaroon Jakmunee). A homemade controller was utilized to control SV_1, SV_2, SV_3, SV_4, SV_5 and P. A degassed unit was used to remove all bubble gases (e.g., CO_2, NH_3 and O_2) that may occur from the reaction. A personal computer with in-house built software (Recorder, version 5) and eDAQ chart software was employed for collecting data and interpreting peak heights, respectively. All tubing for assembling systems were teflon tube of 0.89 mm i.d., except pump tubes.

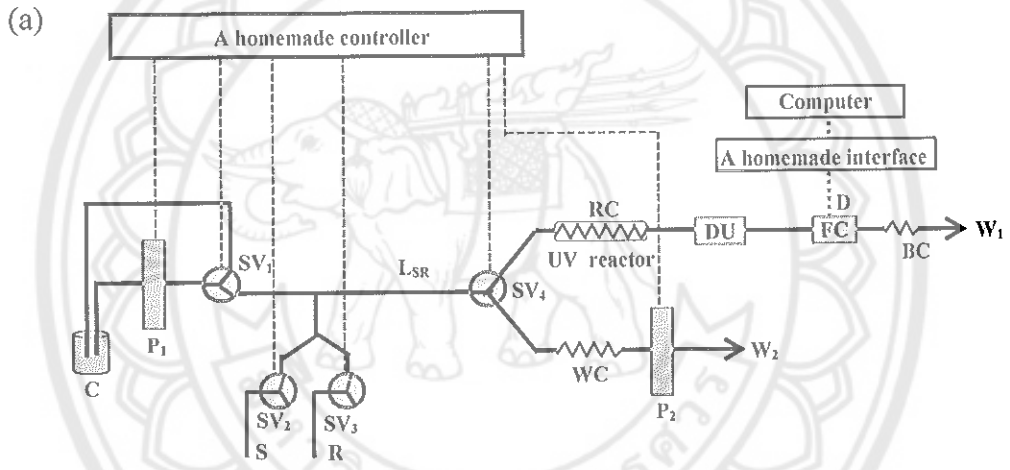

Figure 8 Three designs of the rapid-SAFA spectrophotometric systems with on-line UV photooxidation for COD determination of: (a) system 1, (b) system system 2 and (c) system 3 (C – carrier, R – reagent solution, S – sample/standard solution, L_{SR} – sample and reagent loop, RC – reaction coil, BC – back pressure coil, WC_1 and WC_2 – waste coil 1 and 2 and W_1 and W_2 – waste 1 and 2)

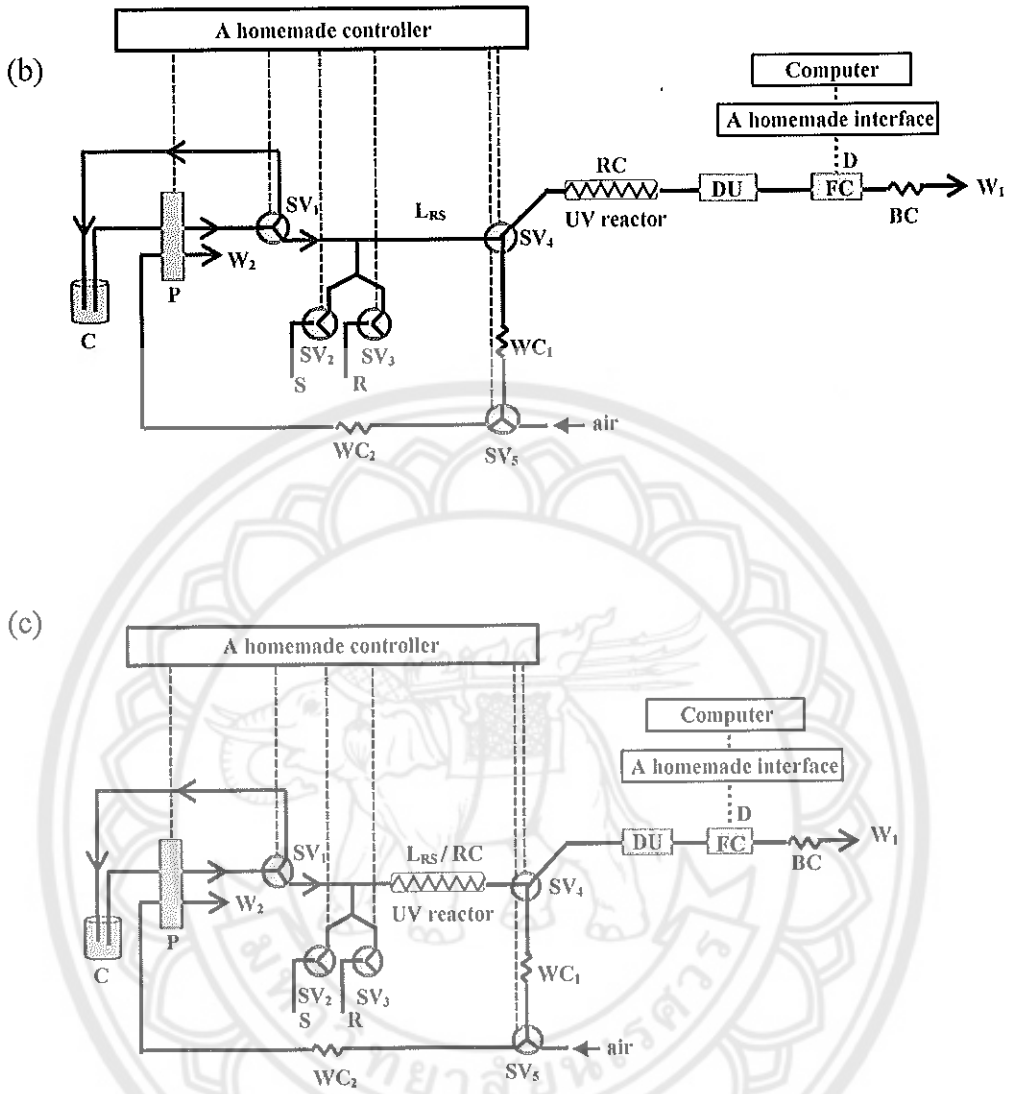

Figure 8 (cont.)

2. Procedure of the system used in this work

In Figure 8 (c) and appendix A1, the system 3 was selected throughout this research. Therefore, the procedure of a rapid-SAFA of system 3 is described as follows. The operation of this system had 4 steps which was consisted of filling, loading, injection and cleaning steps. Firstly, the carrier (C), standard/sample (S) and reagent (R) solutions were filled pass through a L_{SR} (or RC), WC_1, WC_2 and W_2, respectively. After that, the operation cycle of loading and injection steps was started. For the first injection, standard/sample and reagent were rapid sequential aspirated through L_{SR}, WC_1, WC_2 and W_2, respectively. Then, standard/sample plus reagent (S+R) zone in L_{SR} was pushed

and injected to DU, FC of detector and W_1, respectively. Next, the second injection was then started to load and inject according to the operating cycle as above. For the end of analysis, the cleaning step was done to clean L_{SR} and all tubing. As for the procedures of system 1 (Figure 8 (a)) and system 2 (Figure 8 (b)) were similar to system 3 except the different positions of UV reactor and peristaltic pumps.

Determination of COD by the rapid-SAFA spectrophotometric system with on-line UV photooxidation

1. Optimization of the system using acidic $K_2Cr_2O_7$ reagent solution

The key parameters of a rapid-SAFA system using an acidic $K_2Cr_2O_7$ reagent solution were optimized to maximize the oxidation and digestion efficiencies and provided a wide linear range, good linearity and sensitivity, good accuracy and precision. These parameters were 1) standard/sample (V_S) and reagent (V_R) volumes (varied as aspiration times in second of V_S:V_R of 2:1, 2:2, 2:3, 2:4, 3:3 and 4:4), 2) stopped times at UV reactor (varied in the range 0 - 30 s), 3) $K_2Cr_2O_7$ concentrations (varied in the range 0.005 - 0.03 mol L^{-1}), 4) H_2SO_4 concentrations (varied in the range 0.3 - 1.2 mol L^{-1}), 5) $K_2S_2O_8$ concentrations (varied in the range 0 - 4% w/v), 6) carrier solutions (varied in the range 0 - 0.75 mol L^{-1} H_2SO_4), 7) reaction loop lengths at UV reactor (varied in the range 150 - 300 cm), 8) flow rates of carrier (varied in the range 0.8 - 1.4 mL min^{-1}), 9) interference study, 10) digestion efficiency study and 11) analytical characteristic data. Finally, the selected conditions of the proposed system were summarized for the determination of COD in real wastewater samples.

2. Optimization of the system using acidic $KMnO_4$ reagent solution

The main parameters of a rapid-SAFA system using an acidic $KMnO_4$ reagent solution were optimized to also maximize the oxidation and digestion efficiencies and provided a good sensitivity, good linearity, wide linear range, good accuracy and precision. These parameters were 1) $KMnO_4$ concentrations (varied in the range 0.4 - 0.8 mmol L^{-1}), 2) H_2SO_4 concentrations (varied in the range 0.1 - 0.4 mol L^{-1}), 3) standard/sample (V_S) and reagent (V_R) volumes (varied as aspiration times in second of V_S:V_R of 2:1, 3:2 and 4:3), 4) carrier solutions (varied in the range 0 - 0.3 mol L^{-1} H_2SO_4), 5) flow rates of carrier (varied in the range 0.8 - 1.4 mL min^{-1}), 6) reaction loop lengths at UV reactor (varied in the range 150 - 250 cm) and 7) analytical characteristic

data. Finally, the selected conditions of the proposed systems were summarized for the determination of COD in real wastewater samples.

3. Application of the rapid – SAFA system to real wastewater samples

Under optimum conditions of a rapid-SAFA spectrophotometric system, using both acidified $K_2Cr_2O_7$ and $KMnO_4$ based reactions which were applied to determine COD in various sources of wastewater samples. In order to validate of the system, all wastewater samples were added with standard KHP solutions (prepared equivalent to COD concentration) by determining obtained recoveries of the proposed system. Each sample solution was analyzed in triplicate. Results obtained of the proposed systems using both acidified oxidizing agents, were compared with each other and with the standard titration method (see appendix A2) and evaluated by t-test (at 95 % confidence level) and correlation coefficient graphs.

CHAPTER IV

RESULTS AND DISCUSSION

Study of absorption spectra

The absorption spectra were preliminary studied the redox reactions between standard KHP solutions and the acidic $K_2Cr_2O_7$ and $KMnO_4$ reagent solutions prior to COD analysis by a rapid-SAFA system. The study was done in combination with the conventional digestion techniques of a closed reflux and water bath, respectively. For acidified $K_2Cr_2O_7$ based reaction, it was found that the maximum wavelength was 600 nm (shown in Figure 9 (a)). The absorption at 600 nm was represented the increase in color intensity of chromium(III) ion when increase in concentration of standard KHP solutions. Meanwhile, the maximum wavelength at 525 nm was resulted (shown in Figure 9 (b)) when acidified $KMnO_4$ based reaction was used. The absorption at 525 nm was represented the decrease in color intensity of $KMnO_4$ when increase in concentration of standard KHP solutions. Therefore, wavelengths of 600 and 525 nm were selected for COD determination using acidic $K_2Cr_2O_7$ and $KMnO_4$ reagent solutions, respectively, throughout this work.

Design of the rapid-SAFA systems

In order to maximize sensitivity and analysis time of the system. The designed manifolds of system 1, 2 and 3 of the rapid-SAFA spectrophotometry as shown in Figure 8 (a), 8 (b) and 8 (c), respectively, were investigated. It was found that the system 1 and 2 gave lower sensitivity and higher analysis time (8 min per injection) than system 3 (5 min 16 sec per injection) because system 1 and 2 had high dispersion due to long lengths of L_{SR} and RC at UV reactor (shown in Figure 10 (a) and (b)). Therefore, the system 3 was selected to be used throughout this work. The system 3 also offered the usage of one pump and a re-used of carrier solution. Moreover, a L_{SR} or RC (L_{SR}/RC) was placed at UV reactor to reduce dispersion and analysis time.

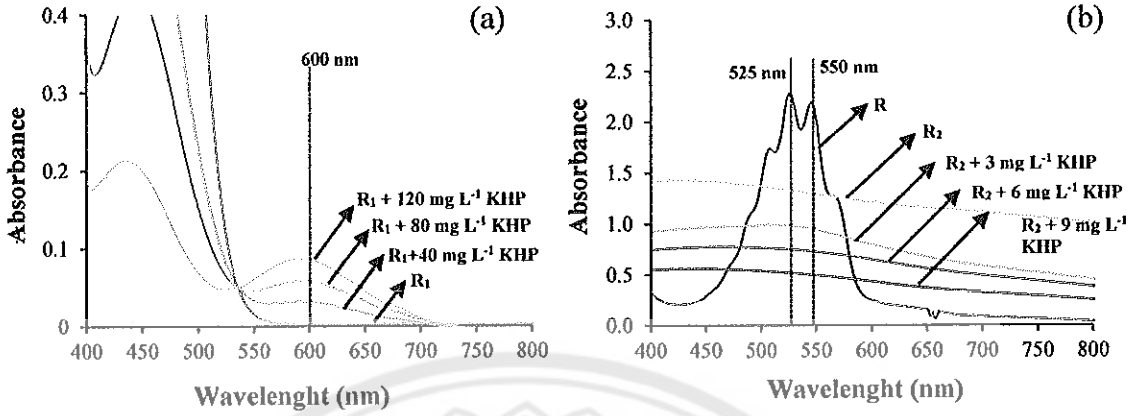

Figure 9 Absorption spectra of: (a) standard KHP solutions (40, 80 and 120 mg L^{-1}) in acidic $K_2Cr_2O_7$ reagent solution (R_1: 0.003 mol L^{-1} $K_2Cr_2O_7$ plus 8.6 mol L^{-1} H_2SO_4) and (b) standard KHP solutions (3, 6 and 9 mg L^{-1}) in acidic $KMnO_4$ reagent solution (R_2: 0.4 mmol L^{-1} $KMnO_4$ plus 0.2 mol L^{-1} H_2SO_4) and a 1×10^{-3} mol L^{-1} $KMnO_4$ solution (R)

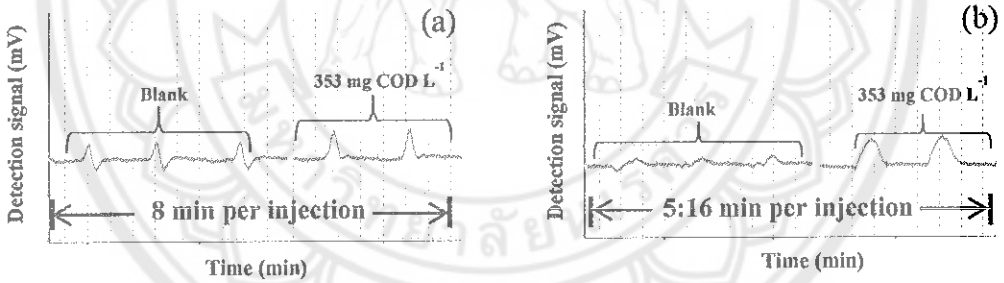

Figure 10 Rapid-SAFA signals for COD determination using three designs of: (a) system 1 and 2 and (b) system 3

Determination of COD by the rapid-SAFA spectrophotometric system with on-line UV photooxidation

1. Optimization of the system using acidic $K_2Cr_2O_7$ reagent solution

Preliminary conditions for COD determination by the rapid-SAFA spectrophotometric system in Figure 8 (c) were used as shown in Table 4. The optmization study of conditions were as following.

Table 4 Preliminary conditions used of the rapid-SAFA spectrophotometric system using acidic $K_2Cr_2O_7$ reagent solution

Parameters	Conditions used
Rapid-SAFA system:	
Reagent solution	0.01 mol L^{-1} $K_2Cr_2O_7$ + 0.5 mol L^{-1} H_2SO_4 + 3% w/v $K_2S_2O_8$
Carrier solution	0.5 mol L^{-1} H_2SO_4
UV reactor	36 W of UV lamp wound with PTFE tubing of 200 cm (i.d. 0.89 mm)
Flow rate	1.0 mL min^{-1}
Stopped time at UV reactor	0 s
Standard/sample and reagent volumes	15 µL and 5 µL (equal to 2 s and 1 s of aspiration times)
Detection wavelength	600 nm
Operation times of the system:	
1) Filling steps of;	
- carrier to UV reactor, FC and W_1	320 s
- reagent to W_2	20 s
- standard/sample to W_2	20 s
2) Loading step of;	
- rapid sequenced aspiration of standard/sample and reagent at L_{SR} to W_2	150 s
3) Injection step of;	
- standard/ sample plus reagent zone at UV reactor to FC and W_1	195 s
4) Cleaning steps of;	
- standard/sample to W_2	60 s
- reagent to W_2	60 s
- carrier to W_2	120 s

1.1 Effect of standard/sample and reagent volumes by mean of aspiration times

In order to maximize sensitivity of the system and to maximize mixing of standard/sample and reagent solutions, the effect of standard/sample (V_S) and reagent (V_R) volumes by mean of aspiration times in seconds was studied. These aspiration times were controlled by a homemade controller. Using the manifold as shown in Figure 8 (c) and preliminary conditions as described in Table 4, blank and standard KHP solutions (300 and 500 mg L^{-1} KHP equivalent to 353 and 558 mg COD L^{-1}) were aspirated into the system. Various standard/sample and reagent volumes (with aspiration time ratios (s:s) of V_S:V_R of 2:1, 2:2, 2:3, 2:4, 3:3 and 4:4) were varied and optimized. Results are shown in Table 5 and Figure 11. It was found that aspiration time ratios of 2:1, 2:2, 2:4, 3:3 and 4:4 s:s were resulted in doublet peaks and the ratios of 3:3 and 4:4 were shown the highest peak height. Thus, the aspirated time of 2 seconds (approximately 15 µL) of standard/sample and 3 seconds (approximately 25 µL) of reagent were chosen as giving suitable peak height and no doublet peak was found.

Table 5 Effect of standard/sample (V_S) and reagent (V_R) volumes by mean of aspiration times (in second) on peak height of standard KHP solutions (equivalent to COD concentrations)

V_S : V_R (s:s)	COD (mg L^{-1})	Peak height (mV)					
		1	2	3	$\bar{X}$	$\bar{X}$- blank	SD
2:1	0 (blank)	0.042	0.044	0.043	0.043	0.000	0.001
	353	0.093	0.094	0.094	0.094	0.051	0.001
	558	0.092	0.093	0.088	0.091	0.048	0.003
2:2	0 (blank)	0.018	0.018	0.016	0.017	0.000	0.001
	353	0.046	0.046	0.044	0.046	0.028	0.001
	558	0.101	0.098	0.094	0.098	0.080	0.004
2:3	0 (blank)	0.010	0.007	0.007	0.008	0.000	0.001
	353	0.029	0.031	0.031	0.030	0.022	0.001
	558	0.089	0.089	0.085	0.088	0.080	0.002

Table 5 (cont.)

$V_S : V_R$ (s:s)	COD (mg L^{-1})	Peak height (mV)					
		1	2	3	$\bar{X}$	$\bar{X}$- blank	SD
2:4	0 (blank)	0.017	0.015	0.013	0.015	0.000	0.002
	353	0.028	0.029	0.029	0.028	0.013	0.001
	558	0.059	0.057	0.059	0.058	0.043	0.001
3:3	0 (blank)	0.012	0.011	0.013	0.012	0.000	0.001
	353	0.055	0.055	0.054	0.055	0.042	0.001
	558	0.111	0.109	0.109	0.109	0.097	0.001
4:4	0 (blank)	0.015	0.015	0.015	0.015	0.000	0.000
	353	0.055	0.057	0.057	0.057	0.042	0.001
	558	0.110	0.110	0.111	0.110	0.096	0.001

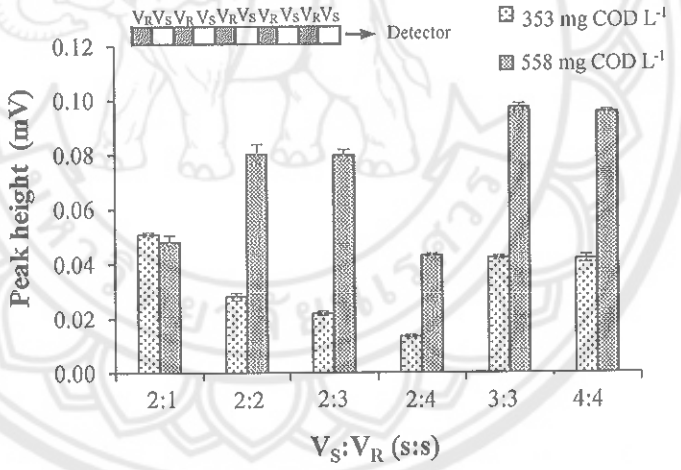

Figure 11 Effect of sample (V_S) and reagent (V_R) volumes by mean of aspiration times (in second) on peak height of standard KHP solutions (300 and 500 mg L^{-1} of KHP equivalent to 353 and 558 mg COD L^{-1})

1.2 Effect of stopped time at UV reactor

Because of the requirement of complete reactions for the oxidation of KHP with acidic $K_2Cr_2O_7$ and digestion using UV photooxidation, the effect of stopped time with time in seconds at UV reactor was studied in order to achieve high sensitivity and high oxidation and digestion efficiency. Various stopped times at UV reactor (0, 2,

5, 10 and 30 s) were varied and optimized. Using obtained conditions in 1.1, blank and standard KHP solutions (300 and 500 mg L^{-1} KHP equivalent to 353 and 558 mgCOD L^{-1}) were aspirated into the system. The results are shown in Table 6 and Figure 12. It was shown that peak heights of 353 and 558 mg COD L^{-1} were slightly decreased when increased the stopped times at UV reactor although high stopped time refers to high oxidation and digestion efficiency. Thus, a stopped time of 0 sec was chosen for further studies as it provide highest peak (with lowest dispersion) although it was lowest oxidation and digestion efficiency but low dispersion. In addition, this selected stopped time of 0 sec was also provided less analysis time (5 minutes 10 seconds or 5:10 min).

Table 6 Effect of stopped time at UV reactor on peak height of standard KHP solutions (equivalent to COD concentrations)

Stopped time (s)	COD (mg L^{-1})	Peak height (mV)					
		1	2	3	$\bar{X}$	$\bar{X}$ - blank	SD
0	0 (blank)	0.005	0.006	0.006	0.006	0.000	0.001
	353	0.039	0.042	0.038	0.039	0.034	0.002
	558	0.111	0.112	0.112	0.112	0.106	0.001
2	0 (blank)	0.006	0.007	0.006	0.007	0.000	0.001
	353	0.037	0.038	0.037	0.037	0.031	0.001
	558	0.114	0.111	0.107	0.111	0.104	0.003
5	0 (blank)	0.007	0.007	0.006	0.007	0.000	0.001
	353	0.031	0.031	0.031	0.031	0.024	0.000
	558	0.109	0.110	0.103	0.107	0.100	0.004
10	0 (blank)	0.007	0.007	0.007	0.007	0.000	0.000
	353	0.028	0.028	0.028	0.028	0.021	0.000
	558	0.100	0.111	0.109	0.107	0.099	0.006
30	0 (blank)	0.006	0.007	0.006	0.007	0.000	0.001
	353	0.023	0.023	0.021	0.022	0.016	0.001
	558	0.088	0.087	0.086	0.087	0.080	0.001

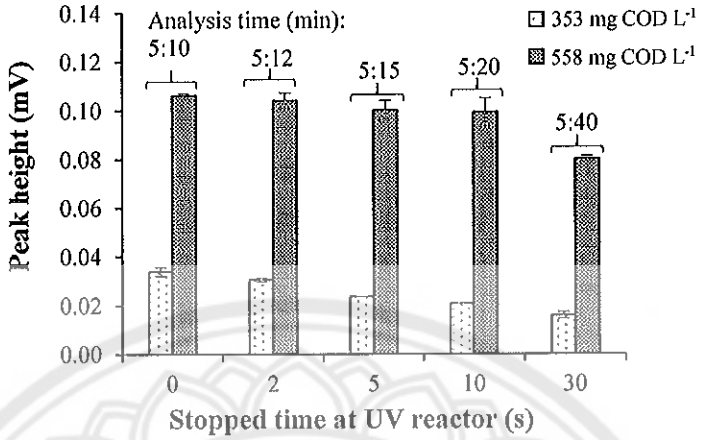

Figure 12 Effect of stopped time at UV reactor on peak height of standard KHP solutions (300 and 500 mg L^{-1} of KHP equivalent to 353 and 558 mg COD L^{-1})

1.3 Effect of $K_2Cr_2O_7$ concentration

A $K_2Cr_2O_7$ is an oxidizing agent to oxidize organic compound and its concentration affects to sensitivity and linearity of the calibration graph. Thus, the effect of $K_2Cr_2O_7$ concentrations was studied. Various concentrations of $K_2Cr_2O_7$ (0.005, 0.01, 0.02, 0.025 and 0.03 mol L^{-1} $K_2Cr_2O_7$) were varied and optimized. Using the obtained conditions in 1.1 and 1.2, blank and standard KHP solutions (100, 200, and 300 mg L^{-1} KHP equivalent to 112, 223 and 353 mg COD L^{-1}) were aspirated into the system. Results are shown in Table 7 and Figure 13. It was found that slopes were decreased with decreasing concentration of $K_2Cr_2O_7$ (lower than 0.25 mol L^{-1}) which were referred to a limitation of stoichiometry. Over concentration of 0.025 mol L^{-1}, a slope was decreased because of high intensity of $K_2Cr_2O_7$ (high blank signal). Therefore, a 0.025 mol L^{-1} $K_2Cr_2O_7$ was chosen for further studies, as it provided highest sensitivity and linearity (r^2 = 0.9992).

Table 7 Effect of $K_2Cr_2O_7$ concentration on peak height and slope of standard KHP solutions (equivalent to COD concentrations)

$K_2Cr_2O_7$ (mol L^{-1})	COD (mg L^{-1})	Peak height (mV)						Slope	r^2
		1	2	3	$\bar{X}$	$\bar{X}$ - blank	SD		
0.005	0 (blank)	0.005	0.005	0.005	0.005	0.000	0.000	6.00×10^{-5}	0.9606
	112	0.009	0.006	0.007	0.007	0.002	0.001		
	223	0.012	0.011	0.011	0.011	0.007	0.001		
	353	0.021	0.020	0.020	0.020	0.015	0.001		
0.010	0 (blank)	0.006	0.006	0.006	0.006	0.000	0.000	1.50×10^{-4}	0.9005
	112	0.011	0.011	0.010	0.011	0.005	0.001		
	223	0.017	0.017	0.018	0.018	0.011	0.001		
	353	0.043	0.043	0.044	0.043	0.037	0.001		
0.020	0 (blank)	0.011	0.011	0.011	0.011	0.000	0.000	2.40×10^{-4}	0.9574
	112	0.017	0.017	0.016	0.017	0.006	0.001		
	223	0.033	0.034	0.034	0.034	0.023	0.001		
	353	0.073	0.072	0.067	0.071	0.060	0.003		
0.025	0 (blank)	0.012	0.012	0.011	0.012	0.000	0.000	3.10×10^{-4}	0.9992
	112	0.022	0.021	0.022	0.022	0.010	0.001		
	223	0.057	0.057	0.057	0.057	0.046	0.000		
	353	0.092	0.089	0.089	0.090	0.078	0.001		
0.030	0 (blank)	0.042	0.042	0.042	0.042	0.000	0.000	1.00×10^{-4}	0.9758
	112	0.059	0.055	0.056	0.057	0.015	0.002		
	223	0.072	0.071	0.070	0.071	0.029	0.001		
	353	0.081	0.078	0.078	0.079	0.037	0.001		

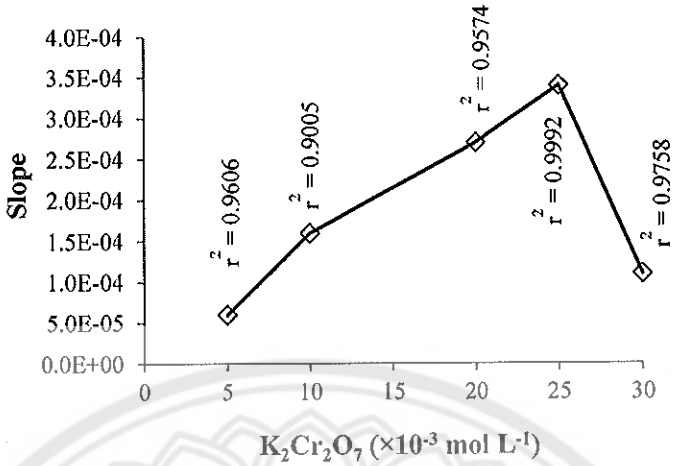

Figure 13 Effect of $K_2Cr_2O_7$ concentration on slope of standard KHP solutions (100 - 300 mg L^{-1} of KHP equivalent to 112 - 353 mg COD L^{-1})

1.4 Effect of H_2SO_4 concentration

Sulfuric acid is one of factors to accelerate the oxidation of organic compound and affect to sensitivity and linearity of the calibration graph. Thus, the effect of H_2SO_4 concentrations (0.3 - 1.2 mol L^{-1}) was studied. Using the obtained conditions in 1.1 - 1.3, blank and standard KHP solutions (100, 150, 200 and 300 mg L^{-1} KHP equivalent to 112, 168, 223 and 353 mg COD L^{-1}) were aspirated into the system. The results are shown in Table 8 and Figure 14. It was shown that the sensitivity decreased when increased the concentration of H_2SO_4. At 0.3 and 0.5 mol L^{-1} H_2SO_4 were resulted in the highest sensitivity but at 0.3 mol L^{-1} H_2SO_4 was found doublet peaks for all COD concentrations. Moreover, the higher H_2SO_4 concentrations than 0.5 mol L^{-1} caused refractive index effect. Thus, a 0.5 mol L^{-1} H_2SO_4 was selected for further studies, as it provided highest sensitivity and good linearity (r^2 = 0.9644) and no effect of refractive index was found.

Table 8 Effect of H_2SO_4 concentration on peak height and slope of standard KHP solutions (equivalent to COD concentrations)

H_2SO_4 (mol L^{-1})	COD (mg L^{-1})	Peak height (mV)						Slope	r^2
		1	2	3	$\bar{X}$	$\bar{X}$ - blank	SD		
0.3	0 (blank)	0.013	0.012	0.013	0.013	0.000	0.000	3.00×10^{-4}	0.9843
	112	0.021	0.018	0.020	0.020	0.007	0.001		
	168	0.037	0.038	0.038	0.037	0.024	0.001		
	223	0.060	0.062	0.059	0.060	0.047	0.002		
	353	0.087	0.085	0.086	0.086	0.073	0.001		
0.5	0 (blank)	0.010	0.011	0.011	0.011	0.000	0.001	3.00×10^{-4}	0.9644
	112	0.020	0.020	0.020	0.020	0.009	0.000		
	168	0.026	0.027	0.027	0.026	0.016	0.001		
	223	0.042	0.042	0.042	0.042	0.031	0.000		
	353	0.082	0.084	0.085	0.084	0.073	0.002		
0.7	0 (blank)	0.023	0.026	0.023	0.024	0.000	0.001	1.40×10^{-4}	0.9549
	112	0.032	0.034	0.034	0.033	0.009	0.001		
	168	0.037	0.038	0.037	0.037	0.013	0.001		
	223	0.044	0.043	0.043	0.043	0.019	0.001		
	353	0.071	0.062	0.061	0.065	0.041	0.005		
0.9	0 (blank)	0.042	0.038	0.043	0.041	0.000	0.003	8.00×10^{-5}	0.9751
	112	0.051	0.050	0.051	0.051	0.010	0.001		
	168	0.053	0.055	0.053	0.053	0.013	0.001		
	223	0.054	0.061	0.056	0.057	0.016	0.004		
	353	0.068	0.068	0.066	0.068	0.027	0.001		
1.2	0 (blank)	0.057	0.061	0.062	0.060	0.000	0.003	5.00×10^{-5}	0.9218
	112	0.073	0.071	0.066	0.070	0.010	0.004		
	168	0.071	0.071	0.071	0.071	0.011	0.000		
	223	0.075	0.072	0.071	0.072	0.012	0.002		
	353	0.079	0.083	0.078	0.080	0.020	0.003		

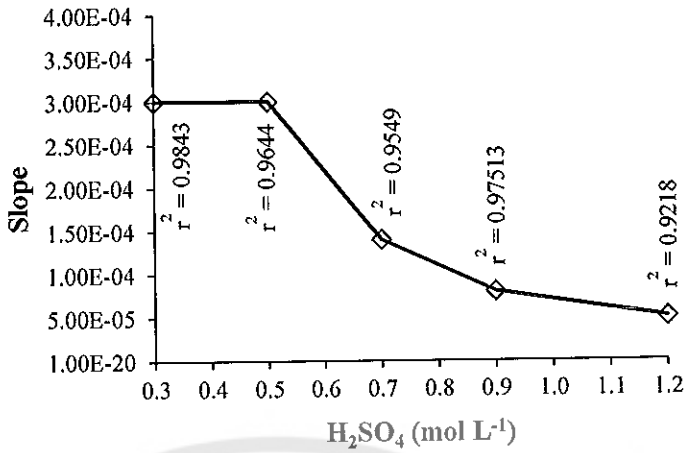

Figure 14 Effect of H_2SO_4 concentration on slope of standard KHP solutions (100 - 300 mg L^{-1} KHP equivalent to 112 - 353 mg COD L^{-1})

1.5 Effect of $K_2S_2O_8$ concentration

The $K_2S_2O_8$ is a strong oxidant and it was acted as a catalytic photooxidation using UV irradiation to produce strong oxidant of free radical such as hydroxy free radical ($OH^{\bullet}$) [33]. Thus, $K_2S_2O_8$ concentration in reagent solution is the most important factor to achieve the highest sensitivity and digestion efficiency for UV photooxidation. The effect of $K_2S_2O_8$ concentrations (0 - 4 % w/v) was studied. Using the obtained conditions in 1.1 - 1.4, blank and standard KHP solutions (150, 200, 250 and 300 mg L^{-1} KHP equivalent to 168, 223, 279 and 353 mg COD L^{-1}) were aspirated into the system. The results in Table 9 and Figure 15 showed that the sensitivity increased when increased concentrations of 1 to 3% w/v $K_2S_2O_8$ and then decreased at 4% w/v of $K_2S_2O_8$. This is due to 4% w/v of $K_2S_2O_8$ was difficult to dissolve in water. Therefore, a 3% w/v of $K_2S_2O_8$ was selected as giving a good sensitivity.

Table 9 Effect of $K_2S_2O_8$ concentration on peak height and slope of standard KHP solutions (equivalent to COD concentrations)

$K_2S_2O_8$ (%w/v)	COD (mg L^{-1})	Peak height (mV)						Slope	r^2
		1	2	3	$\bar{X}$	$\bar{X}$ - blank	SD		
0	0 (blank)	0.029	0.029	0.028	0.029	0.000	0.001	1.00×10^{-5}	0.9000
	168	0.044	0.045	0.044	0.044	0.015_5	0.001		
	223	0.044	0.045	0.045	0.045	0.015_8	0.002		

Table 9 (cont.)

$K_2S_2O_8$ (%w/v)	COD (mg L^{-1})	Peak height (mV)						Slope	r^2
		1	2	3	$\bar{X}$	$\bar{X}$ - blank	SD		
	279	0.045	0.045	0.046	0.046	0.016_{70}	0.001		
	353	0.045	0.046	0.045	0.046	0.016_{73}	0.001		
	0 (blank)	0.011	0.011	0.011	0.011	0.000	0.000		
	168	0.039	0.039	0.037	0.038	0.027	0.001		
2	223	0.057	0.057	0.060	0.058	0.047	0.001	2.20×10^{-4}	0.9206
	279	0.070	0.070	0.072	0.070	0.059	0.001		
	353	0.076	0.076	0.072	0.074	0.063	0.002		
	0 (blank)	0.012	0.012	0.012	0.012	0.000	0.000		
	168	0.027	0.027	0.026	0.026	0.014	0.001		
3	223	0.035	0.035	0.037	0.036	0.024	0.001	2.80×10^{-4}	0.9767
	279	0.053	0.053	0.055	0.053	0.041	0.001		
	353	0.075	0.073	0.072	0.073	0.061	0.001		
	0 (blank)	0.020	0.020	0.020	0.020	0.000	0.000		
	168	0.028	0.027	0.026	0.027	0.007	0.001		
4	223	0.033	0.032	0.032	0.032	0.013	0.001	2.00×10^{-4}	0.9372
	279	0.043	0.043	0.043	0.043	0.023	0.000		
	353	0.061	0.061	0.061	0.061	0.042	0.000		

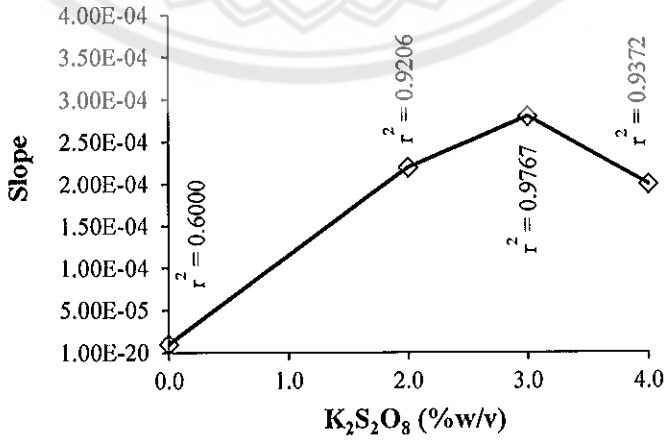

Figure 15 Effect of $K_2S_2O_8$ concentration on slope of standard KHP solutions (150 - 300 mg L^{-1} of KHP equivalent to 168 - 353 mg COD L^{-1})

1.6 Effect of carrier solution using H_2SO_4

The influence of the schlieren effect may occur in liquid media that affect on analytical signal of flow analysis, especially in single line manifold. The effect of carrier stream concentrations using H_2SO_4 was examined in order to reduce refractive index of all peaks and blank signal. Various H_2SO_4 concentrations (0, 0.25, 0.5 and 0.75 mol L^{-1}) of carrier stream were varied and optimized. Using the obtained condition in 1.1 - 1.5, blank and standard KHP solutions (150, 200, 250 and 300 mg L^{-1} KHP equivalent to 168, 223, 279 and 353 mg COD L^{-1}) were aspirated into the system. Results in Table 10 and Figure 16 show that the sensitivity increased when increased concentrations of H_2SO_4 up to 0.5 mol L^{-1} and then decreased at 0.75 mol L^{-1} of H_2SO_4. All these concentrations, except 0.5 mol L^{-1}, were different density between reagent and carrier solutions and resulted refractive index of all peaks. Therefore, a 0.5 mol L^{-1} H_2SO_4 was selected as it giving a good sensitivity and low noise signal of blank and no refractive index was found.

Table 10 Effect of carrier solution using H_2SO_4 on peak height and slope of standard KHP solutions (equivalent to COD concentrations)

Carrier solution using H_2SO_4 (mol L^{-1})	COD (mg L^{-1})	Peak height (mV)						Slope	r^2
		1	2	3	$\bar{X}$	$\bar{X}$ - blank	SD		
0	0 (blank)	0.077	0.076	0.070	0.074	0.000	0.004	1.70×10^{-4}	0.9907
	168	0.076	0.078	0.078	0.077	0.003	0.001		
	223	0.084	0.085	0.084	0.085	0.011	0.001		
	279	0.093	0.094	0.095	0.094	0.020	0.001		
	353	0.106	0.107	0.103	0.105	0.031	0.003		
0.25	0 (blank)	0.040	0.040	0.042	0.041	0.000	0.001	2.00×10^{-4}	0.9877
	168	0.045	0.045	0.045	0.045	0.004	0.000		
	223	0.053	0.053	0.054	0.053	0.012	0.001		
	279	0.065	0.065	0.065	0.065	0.024	0.000		
	353	0.078	0.078	0.077	0.078	0.037	0.001		

Table 10 (cont.)

carrier solution using H_2SO_4 (mol L^{-1})	COD (mg L^{-1})	Peak height (mV)						Slope	r^2
		1	2	3	$\bar{X}$	$\bar{X}$ - blank	SD		
0.50	0 (blank)	0.011	0.011	0.011	0.011	0.000	0.000	3.20×10^{-4}	0.9984
	168	0.027	0.027	0.027	0.027	0.016	0.000		
	223	0.045	0.045	0.045	0.045	0.034	0.000		
	279	0.064	0.066	0.0654	0.065	0.054	0.001		
	353	0.081	0.079	0.082	0.081	0.070	0.001		
0.75	0 (blank)	0.045	0.044	0.046	0.045	0.000	0.001	1.70×10^{-4}	0.9986
	168	0.056	0.056	0.056	0.056	0.011	0.000		
	223	0.064	0.065	0.067	0.065	0.020	0.002		
	279	0.076	0.077	0.076	0.076	0.031	0.001		
	353	0.083	0.089	0.079	0.084	0.039	0.005		

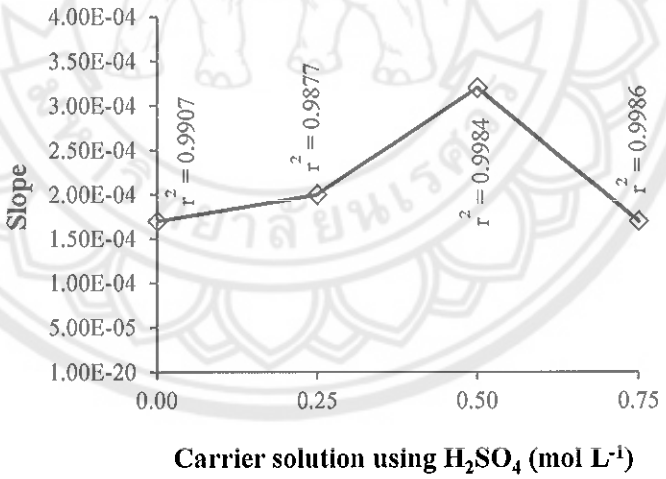

Figure 16 Effect of carrier solution using H_2SO_4 on slope of standard KHP solutions (150 - 300 mg L^{-1} of KHP equivalent to 168 - 353 mg COD L^{-1})

1.7 Effect of reaction loop length at UV reactor

The reaction loop (L_{SR}) length is a parameter affecting dispersion and sample or reagent volume in L_{RS}. This parameter could affect the sensitivity, digestion

efficiency for UV photooxidation, and analysis time of the system. The effect of reaction loop lengths (150-300 cm) were studied. Using the obtained conditions in 1.1 - 1.6, blank and standard KHP solutions (150, 200, 250 and 300 mg L^{-1} KHP equivalent to 168, 223, 279 and 353 mg COD L^{-1}) were aspirated into the system. Results are shown in Table 11 and Figure 17. It was found that a shorter loop length than 200 cm was resulted lower sensitivity because of low total sample and reagent volumes. At reaction loop over 250 cm, the sensitivity were decreased due to slightly dispersion. Therefore, a reaction coil length (L_{SR}) of 200 cm was chosen, as it provided the highest sensitivity and sharp peak and gave less analysis time of 5 minutes 10 seconds (or 5:10 min).

Table 11 Effect of reaction loop length at UV reactor on peak height and slope of standard KHP solutions (equivalent to COD concentrations)

Reaction loop length (cm)	COD (mg L^{-1})	Peak height (mV)						Slope	r^2
		1	2	3	$\bar{X}$	$\bar{X}$ - blank	SD		
150	0 (blank)	0.011	0.011	0.010	0.011	0.000	0.001	2.20×10^{-4}	0.9966
	168	0.023	0.026	0.024	0.024	0.014	0.001		
	223	0.034	0.034	0.035	0.035	0.024	0.001		
	279	0.048	0.048	0.050	0.048	0.038	0.001		
	353	0.060	0.061	0.062	0.061	0.050	0.001		
200	0 (blank)	0.011	0.011	0.010	0.011	0.000	0.000	3.10×10^{-4}	0.9998
	168	0.027	0.028	0.027	0.027	0.016	0.001		
	223	0.044	0.045	0.045	0.045	0.034	0.001		
	279	0.064	0.064	0.061	0.063	0.052	0.001		
	353	0.078	0.081	0.079	0.079	0.068	0.001		
250	0 (blank)	0.011	0.011	0.011	0.011	0.000	0.000	3.00×10^{-4}	0.9754
	168	0.022	0.022	0.022	0.022	0.010	0.000		
	223	0.033	0.033	0.033	0.033	0.022	0.000		
	279	0.050	0.050	0.048	0.049	0.038	0.001		
	353	0.072	0.072	0.072	0.072	0.061	0.000		
300	0 (blank)	0.009	0.010	0.010	0.009	0.000	0.006	2.30×10^{-4}	0.9439
	168	0.020	0.017	0.017	0.018	0.009	0.001		
	223	0.024	0.026	0.028	0.026	0.017	0.002		

Table 10 (cont.)

Reaction loop length (cm)	COD (mg L^{-1})	Peak height (mV)						Slope	r^2
		1	2	3	$\bar{X}$	$\bar{X}$ - blank	SD		
	279	0.037	0.037	0.034	0.036	0.026	0.001		
	353	0.056	0.056	0.059	0.057	0.048	0.001		

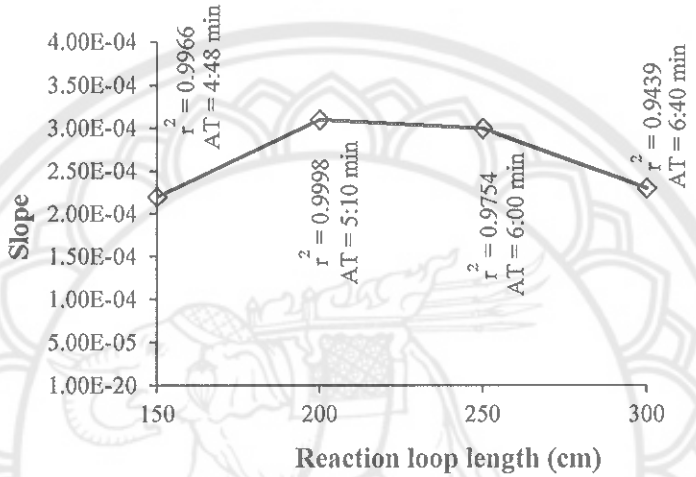

Figure 17 Effect of reaction loop length at UV reactor on slope of standard KHP solutions (150 - 300 mg L^{-1} of KHP equivalent to 168 - 353 mg COD L^{-1}), when AT is analysis time.

1.8 Effect of flow rate

In order to achieve high sensitivity, digestion efficiency and rapid analysis time, the effect of flow rate of carrier was examined. Various flow rate (0.8 - 1.4 mL min^{-1}) was studied. Using the obtained conditions in 1.1-1.7, blank and standard KHP solutions (150, 200, 250 and 300 mg L^{-1} KHP equivalent to 168, 223, 279 and 353 mg COD L^{-1}) were aspirated into the system. Table 12 and Figure 18 showed that the highest sensitivity and maximum of digestion was found at flow rate of 0.8 mL min^{-1}, but it gave long analysis time (5:20 min). At the high flow rate of 1.4 mL min^{-1} was resulted a short analysis time (4:10 min) but low sensitivity was observed because of low digestion efficiency and low dispersion. Thus, the flow rate of 1.0 mL min^{-1} was selected as it provided the highest slope and acceptable analysis time (5:10 seconds).

Table 12 Effect of flow rate on peak height and slope of standard KHP solutions (equivalent to COD concentrations)

Flow rate (mL min^{-1})	COD (mg L^{-1})	Peak height (mV)						Slope	r^2
		1	2	3	$\bar{X}$	$\bar{X}$ - blank	SD		
0.8	0 (blank)	0.013	0.013	0.013	0.013	0.000	0.000	3.30×10^{-4}	0.9983
	168	0.023	0.024	0.026	0.024	0.011	0.001		
	223	0.042	0.042	0.042	0.042	0.028	0.000		
	279	0.060	0.060	0.059	0.059	0.046	0.001		
	353	0.079	0.079	0.081	0.080	0.066	0.001		
1.0	0 (blank)	0.013	0.013	0.013	0.013	0.000	0.000	3.10×10^{-4}	0.9909
	168	0.033	0.034	0.035	0.034	0.021	0.001		
	223	0.053	0.055	0.054	0.054	0.040	0.001		
	279	0.073	0.073	0.073	0.073	0.060	0.000		
	353	0.084	0.087	0.087	0.086	0.072	0.001		
1.2	0 (blank)	0.015	0.015	0.015	0.015	0.000	0.000	3.00×10^{-4}	0.9951
	168	0.031	0.031	0.031	0.031	0.016	0.000		
	223	0.045	0.045	0.044	0.045	0.030	0.001		
	279	0.066	0.065	0.065	0.065	0.050	0.001		
	353	0.079	0.079	0.081	0.080	0.065	0.001		
1.4	0 (blank)	0.016	0.016	0.016	0.016	0.000	0.000	2.40×10^{-4}	0.9997
	168	0.031	0.032	0.032	0.031	0.015	0.001		
	223	0.044	0.044	0.044	0.044	0.028	0.000		
	279	0.059	0.059	0.056	0.058	0.042	0.001		
	353	0.072	0.070	0.071	0.071	0.055	0.001		

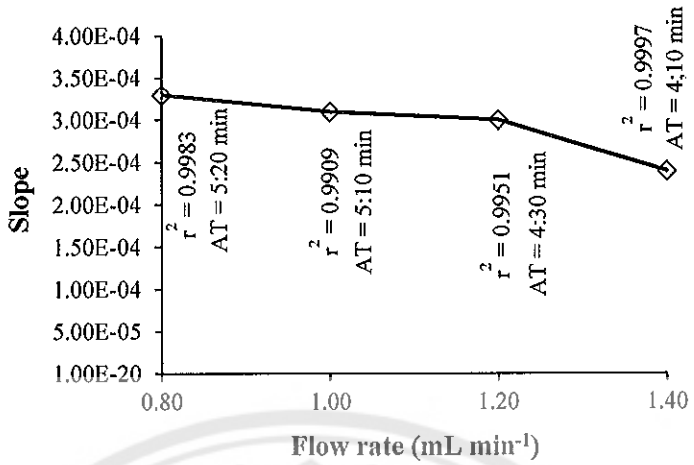

Figure 18 Effect of flow rate on slope of standard KHP solutions (150 – 300 mg L^{-1} of KHP equivalent to 168 - 353 mg COD L^{-1}), when AT is analysis time.

1.9 Effect of digestion efficiency of the system using acidic $K_2Cr_2O_7$ reagent solution

1.9.1 Digestion efficiency study using some model organic compounds

Digestion efficiency of the system using model organic compounds was studied in order to evaluate the digestion efficiency of UV photooxidation reaction. Model organic compounds such as KHP, glucose, benzoic acid, gallic acid, sorbic acid and citric acid in all concentration of 250 mg COD L^{-1} were tested under the optimum conditions in 1.1 – 1.8. The results are shown in Table 13 and Figure 19 (a). It was found that the peak height of glucose, benzoic acid and gallic acid were equal to KHP while ascorbic and citric acids were lower peak heights. These results indicated that glucose, benzoic acid and gallic acid were similarly digested with UV irradiation conditions (36W of UV lamp + 3% w/v $K_2S_2O_8$) because of their similar chemical structures. In order to achieve the high digestion efficiency, model organic compounds of KHP, glucose, benzoic acid and gallic acid should be represents a sensitivity by calibration curve. Under the optimum conditions in 1.1 – 1.8, each of organic compounds in concentrations of 150, 175, 200, 250 and 300 mg COD L^{-1} were aspirated into the system. Results are shown in Table 14 and Figure 19 (b). The calibration graphs of KHP, glucose, benzoic acid and gallic acid were provided similar

sensitivity (slope) and the digestion efficiency percentages were obtained in the range 100-113% (calculated as the ratio of the slope of model organic compound and slope of KHP standard). It indicated that for the proposed system, other models of organic compound, glucose, benzoic acid and gallic acid could be used as COD standard solution instead of KHP solution.

Table 13 Peak height results of digestion efficiency of some model organic compounds by the rapid-SAFA system using acidic $K_2Cr_2O_7$ reagent solution

Model organic compound	Peak height (mV)					
	1	2	3	$\bar{X}$	$\bar{X}$ - blank	SD
blank	0.054	0.055	0.055	0.055	0.000	0.001
KHP	0.112	0.117	0.118	0.116	0.061	0.003
Glucose	0.109	0.110	0.115	0.111	0.057	0.003
Sodium benzoic	0.114	0.117	0.116	0.116	0.061	0.002
Gallic acid	0.113	0.112	0.111	0.112	0.058	0.001
Sorbic acid	0.079	0.076	0.077	0.077	0.023	0.002
Citric acid	0.092	0.092	0.089	0.091	0.036	0.001

Table 14 Analytical characteristic data of some model organic compounds from the study of digestion efficiency

Model organic compound	Linear range (mg COD L^{-1})	Linear equation (y = ax+b)	r^2	%RSD (n=3)	Digestion efficiency (%) *
KHP	150 – 300	y = 0.0004x – 0.0383	0.9932	2.1-10.6	100
Glucose	150 – 300	y = 0.0004x – 0.0432	0.9881	0.9-8.9	100
Sodium benzoate	150 – 300	y = 0.0005x – 0.0470	0.9909	2.8-8.5	113
Gallic acid	150 – 300	y = 0.0004x – 0.0379	0.9986	2.1-14.6	105

$$* \text{ \% Digestion efficiency} = \left[\frac{\text{Slope of model organic compound}}{\text{Slope of KHP}} \right] \times 100$$

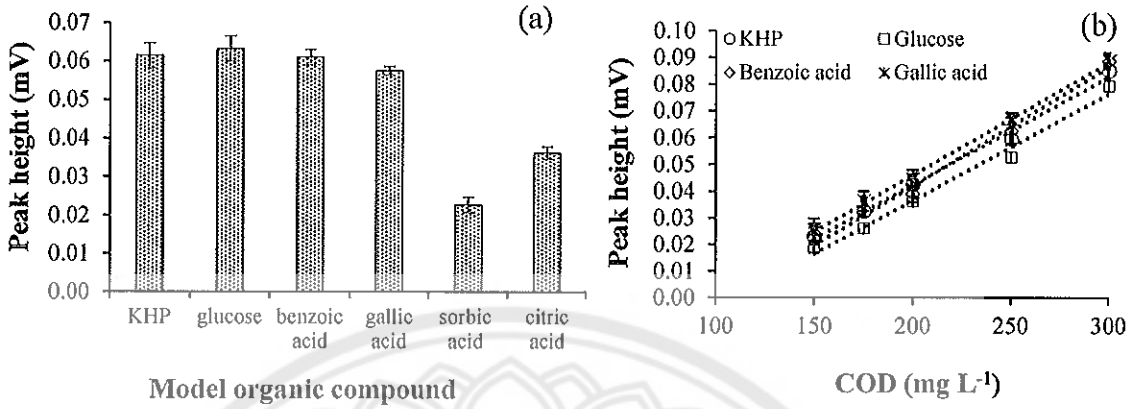

Figure 19 Effect of digestion efficiency on: (a) peak heights (250 mg COD L^{-1}, n = 3) and (b) calibration graphs of some model organic compounds by the rapid-SAFA system using acidic $K_2Cr_2O_7$ reagent solution

1.9.2 Digestion efficiency using mixed standard solutions of some model organic compounds

A mixed standard solution of model organic compounds of KHP, glucose, benzoic acid and gallic acid were used to validate UV photooxidation of the proposed system by determining the resulted recovery. A mixed standard solution of organic compounds including its individual concentrations, was prepared by added KHP, glucose, benzoic acid and gallic acid into water and aspirated into the system using optimum conditions in 1.1 – 1.8. The results are shown in Table 15. It was found that the total concentrations of all samples were closed to the added solutions. And the efficiency of UV photooxidation of the proposed system was good with recoveries in range of 80-103%.

Table 15 COD contents and recoveries of some model organic compounds by the rapid-SAFA system

No.	Model organic compound (mg COD L^{-1})				Total organic compounds (mg COD L^{-1}), n=3			
	KHP	Glucose	Sodium benzoate	Gallic acid	Added	Found ($\bar{X}$±SD)	% RSD	Recovery (%)
1	180	-	-	-	180	186±7	3.8	103±4
2	-	50	-	-	50	47±4	8.5	94±9
3	-	-	50	-	50	43±1	2.3	86±5
4	-	-	-	50	50	40±0	0	80±0
5	180	50	-	-	230	226±7	3.1	98±3
6	180	-	50	-	230	211±4	1.9	92±2
7	180	-	-	50	230	216±10	4.6	94±4
8	180	50	50	-	280	278±2	0.7	99±1
9	180	50	-	50	280	282±6	2.1	101±2
10	180	-	50	50	280	273±6	2.2	98±2

1.9.3 Digestion efficiency study by on-line UV photooxidation and conventional digestion using some model organic compounds

In order to achieve good digestion efficiency the proposed system, an on-line UV photooxidation was compared with a conventional digestion by closed reflux. The concentration of KHP, glucose, gallic acid and benzoic acid equivalent to 294, 267, 282 and 500 mg COD L^{-1} were prepared and digested by 2 digestion methods. And then, the digested solutions were injected by manual direct injection to the FIA system. The results are shown in Table 16. It was resulted that the percentage of digestion efficiency by on-line UV photooxidation were 46, 44, 46 and 43 of KHP, glucose, gallic acid and benzoic acid, respectively. The percentage digestion efficiency were calculated as the ratio of the peak height of each model organic compound by on-line UV photooxidation method and by conventional digestion. These results indicated that the digestion efficiency of an on-line UV photooxidation was less than a closed reflux method approximately 0.43-0.46 times.

Table 16 Digestion efficiency by on-line UV photooxidation and conventional digestion on peak height of some model organic compounds

Model organic compound (mg COD L^{-1})	Peak height (mV); n=3		Digestion efficiency (%)*
	On-line UV photooxidation	Conventional digestion (Closed reflux)	
KHP (294 mg COD L^{-1})	0.273±0.05	0.592±0.01	46
Glucose (267 mg COD L^{-1})	0.234±0.03	0.534±0.00	44
Gallic acid (282 mg COD L^{-1})	0.293±0.01	0.638±0.01	46
Sorbic acid (500 mg COD L^{-1})	0.313±0.03	0.723±0.01	43

$$* \% \text{ Digestion efficiency} = \left[\frac{\text{Peak height of model organic compound by on-line UV photooxidation}}{\text{Peak height of model organic compound by conventional digestion}} \right] \times 100$$

1.10 Interference study

The effect of interference compounds that may found in water sample, were studied. Some interference compounds includes Cl^-, ferrous ion (Fe^{2+}), ferric ion (Fe^{3+}), Nitrite (NO_2^-) and Nitrate (NO_3^-) were used in the proposed study. Using the optimum conditions in 1.1 – 1.8, blank and 250 mg COD L^{-1} were added with various inference solutions with various concentrations of Cl^- (50, 100, 150, 250, 500 and 1000 mg L^{-1}), Fe^{2+} (100 mg L^{-1}) and Fe^{3+} (100 mg L^{-1}), NO_2^- (50 mg L^{-1}) and NO_3^- (50 mg L^{-1}) and were aspirated into the system. The results are shown in Table 17. It was found that the seriously interference of chloride for the determination of COD of the proposed system was tolerated up to 150 mg L^{-1} of Cl^- as defined the relative error of $< \pm$ 10% in the signal of 292 mg COD L^{-1}. No interference were found for Fe^{2+}, Fe^{3+}, NO_2^- and NO_3^- because these ions were found at low concentration in water sample.

Table 17 Effect of interference on peak height of 292 mg COD L^{-1} (equivalent to 250 mg L^{-1} KHP); mean of triplicate injections

Interference compounds	Concentration added (mg L^{-1})	Peak height (mV)*	%Relative error**
none	-	0.085	-
Cl^-	100	0.084	-0.33
	150	0.076	-9.62
	250	0.052	-37.98
	500	0.037	-56.25
	1000	0.035	-58.17
Fe^{3+}	100	0.088	4.30
Fe^{2+}	100	0.084	-0.97
NO_2^-	50	0.087	2.87
NO_3^-	50	0.079	-6.75

* Peak height was corrected from blank signal (blank = 0.068 V)

** %Relative error = $\left[\frac{\text{(Peak height of 292 mg COD } L^{-1} \text{ plus interference) -- (Peak height of 292 mg COD } L^{-1})}{\text{Peak height of 292 mg COD } L^{-1}}\right] \times 100$

1.11 Summary of conditions used of the system using acidic $K_2Cr_2O_7$ reagent solution

The rapid-SAFA spectrophotometric system with on-line UV photooxidation using acidified $K_2Cr_2O_7$ based reactions is depicted in Figure 8 (c) and the optimum conditions are summarized in Table 18.

Table 18 Conditions used of the system using acidic $K_2Cr_2O_7$ reagent solution

Parameters	Conditions used
Rapid-SAFA system:	
Reagent solution	0.025 mol L^{-1} $K_2Cr_2O_7$ + 0.5 mol L^{-1} H_2SO_4 + 3% w/v $K_2S_2O_8$
Carrier solution	0.5 mol L^{-1} H_2SO_4
UV reactor	36 W of UV lamp wound with PTFE tubing of 200 cm (i.d. 0.89 mm)
Flow rate	1.0 mL min^{-1}

Table 18 (cont.)

Parameters	Conditions used
Rapid-SAFA system:	
Stopped time at UV reactor	0 s
Standard/sample and reagent volumes	15 µL and 25 µL (equal to 2 s and 3 s of aspiration times)
Detection wavelength	600 nm
Operation times of the system:	
1) Filling steps of;	
- carrier to UV reactor, FC and W_1	320 s
- reagent to W_2	20 s
- standard/sample to W_2	20 s
2) Loading step of;	
- rapid sequenced aspiration of standard/sample and reagent at L_{SR} to W_2	150 s
3) Injection step of;	
- standard/ sample plus reagent zone at UV reactor to FC and W_1	195 s
4) Cleaning steps of;	
- standard/sample to W_2	60 s
- reagent to W_2	60 s
- carrier to W_2	120 s

1.12 Analytical characteristic data of the system using acidic $K_2Cr_2O_7$ reagent solution

Using the system as shown in Figure 8 (c) and the optimum conditions described in 1.11, blank and standard KHP solutions (25, 50, 75, 100, 125, 150, 175, 200, 250 and 300 mg L^{-1} KHP equivalent to 29, 59, 88, 118, 147, 176, 206, 235, 294 and 353 mg COD L^{-1}) were aspirated into the system. Under the optimum conditions, the results are shown in Table 19 and Figure 20. Linear ranges were obtained in the range of 29 - 176 mg COD L^{-1} (25 - 150 mg L^{-1} KHP) and 176 - 353 mg COD L^{-1} (150 - 300 mg L^{-1} KHP) with linear equations of $y = 0.0001x - 0.0024$ ($r^2 = 0.9911$) and

$y = 0.0003x - 0.0429$ ($r^2 = 0.9957$), respectively. The limit of detection (LOD) were 27 mg COD L^{-1} (23 mg L^{-1} KHP) and 117 mg COD L^{-1} (100 mg L^{-1} KHP). The Limit of detection (LOD) was defined as 3 times of standard deviation of the blank ($LOD = \bar{X} + 3SD_{blank}$). The relative standard deviation (RSD) was in the range of 0 - 7.9 % and the sample throughput was 12 injections per hour.

Table 19 Calibration data of the system for COD determination using acidic $K_2Cr_2O_7$ reagent solution

COD (mg L^{-1})	Peak height (mV)						
	1	2	3	$\bar{X}$	SD	%RSD	$\bar{X}$ - blank
0 (blank)	0.013	0.013	0.012	0.013	0.001	7.9	0.000
29	0.014	0.014	0.014	0.014	0.000	0	0.001
59	0.016	0.016	0.016	0.016	0.000	0	0.003
88	0.018	0.018	0.018	0.018	0.000	0	0.005
118	0.020	0.020	0.022	0.020	0.001	5.0	0.007
147	0.022	0.023	0.023	0.023	0.001	4.4	0.010
176	0.028	0.026	0.026	0.026	0.001	3.9	0.013
206	0.033	0.033	0.032	0.033	0.001	3.0	0.020
235	0.040	0.042	0.042	0.041	0.001	2.4	0.028
294	0.059	0.061	0.061	0.060	0.001	1.7	0.047
353	0.081	0.081	0.078	0.080	0.001	1.3	0.067

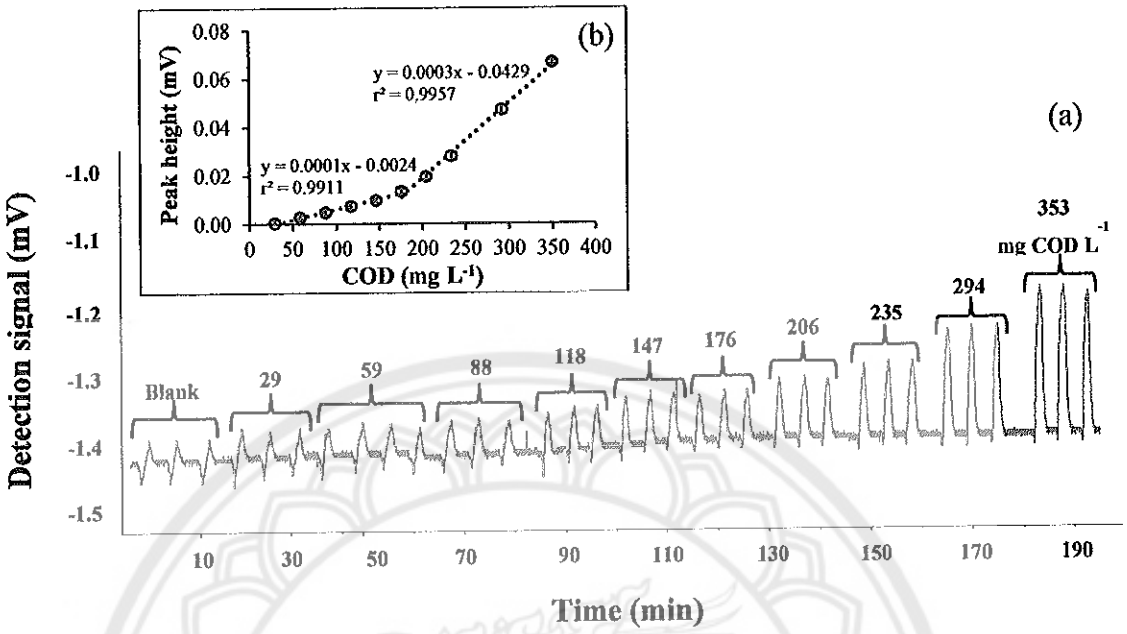

Figure 20 (a) Typical of a rapid-SAFA signals and (b) calibration graph for COD determination using acidic $K_2Cr_2O_7$ reagent solution

2. Optimization of the system using acidic $KMnO_4$ reagent solution

Preliminary conditions for COD determination by the rapid SAFA spectrophotometric system in Figure 8 (c) were used as shown in Table 20. The optmization study of conditions were as following.

Table 20 Preliminary conditions used of the rapid-SAFA spectrophotometric system using acidic $KMnO_4$ reagent solution

Parameters	Conditions used
Rapid-SAFA system:	
Reagent solution	0.8 mmol L^{-1} $KMnO_4$ + 0.3 mol L^{-1} H_2SO_4
Carrier solution	0.3 mol L^{-1} H_2SO_4
UV reactor	36 W of UV lamp wound with PTFE tubing of 200 cm (i.d. 0.89 mm)
Flow rate	1.0 mL min^{-1}
Stopped time at UV reactor	0 s

Table 20 (cont.)

Parameters	Conditions used
Rapid-SAFA system:	
Standard/sample and reagent volumes	15 µL and 25 µL (equal to 2 s and 3 s of aspiration times)
Detection wavelength	525 nm
Operation times of the system:	
1) Filling steps of;	
- carrier to UV reactor, FC and W_1	320 s
- reagent to W_2	20 s
- standard/sample to W_2	20 s
2) Loading step of;	
- rapid sequenced aspiration of standard/sample and reagent at L_{SR} to W_2	150 s
3) Injection step of;	
- standard/ sample plus reagent zone at UV reactor to FC and W_1	300 s
4) Cleaning steps of;	
- standard/sample to W_2	60
- reagent to W_2	60
- carrier to W_2	120

2.1 Stability study of acidic $KMnO_4$ reagent solution

Because of the instability of acidified $KMnO_4$ reagent solution, the stability of this reagent (0.4 mmol L^{-1} $KMnO_4$ in 0.2 mol L^{-1} H_2SO_4) was necessarily studied for the COD determination by using a rapid-SAFA system. The results are shown in Table 21 and Figure 21. This reagent solution slightly decreased its intensity at 25±2 °C and stabilized at 12±2 °C within 180 min. Therefore, the preservation of this reagent at 12±2 °C in ice container was chosen along the research and the experiment of a rapid-SAFA system was carried out within 180 min.

Table 21 Stability study of acidic $KMnO_4$ reagent solution on peak height of standard KHP solution (equivalent to 4 mg COD L^{-1})

Time (min)	Peak height (mV)		Time (min)	Peak height (mV)	
	25±2 °C	12±2 °C		25±2 °C	12±2 °C
6	1.70	0.73	96	1.19	0.84
12	1.71	0.73	102	1.15	0.85
18	1.67	0.73	120	1.11	0.87
24	1.58	0.76	126	1.08	0.87
30	1.53	0.76	132	1.05	0.90
60	1.33	0.87	150	1.06	0.87
78	1.20	0.89	156	1.03	0.85
90	1.19	0.88	180	1.02	0.85

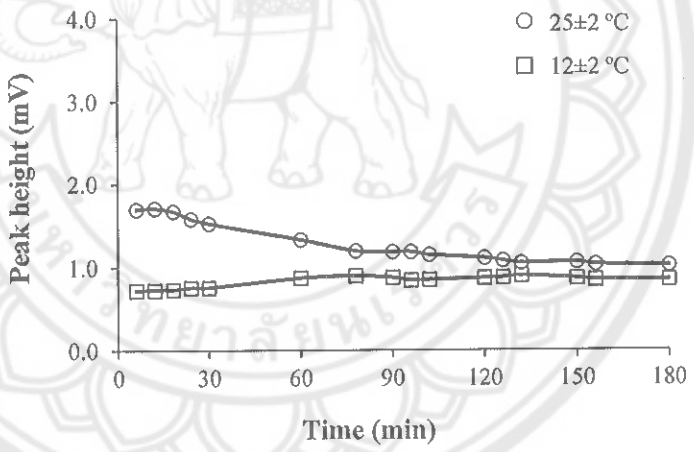

Figure 21 Stability study of acidic $KMnO_4$ reagent solution (0.2 mmol L^{-1} $KMnO_4$ in 0.2 mol L^{-1} H_2SO_4) at 25±2 °C and 12±2 °C by the rapid-SAFA system

2.2 Effect of $KMnO_4$ concentration

The $KMnO_4$ in reagent solution acts as oxidizing agent to oxidize organic compound. It concentration affected to sensitivity and linearity of the calibration graph. Thus, the effect of $KMnO_4$ concentration was studied. Various concentrations of $KMnO_4$ (0.4 - 0.8 mmol L^{-1}) were varied and optimized. Using the manifold and preliminary conditions as shown in Figure 8 (c) and Table 20, respectively. Blank and standard KHP solutions (10, 20, 30 and 50 mg L^{-1} KHP equivalent to 12, 24, 35, 59

mg COD L^{-1}) were aspirated into the system. Results in Table 22 and Figure 22 show that 6×10^{-4} and 8×10^{-4} mol L^{-1} $KMnO_4$ resulted in a wide range of calibration graph but produced precipitated along the system of manganese dioxide (MnO_2) compound. In order to avoid MnO_2 precipitated which may block in the system, a 4×10^{-4} mol L^{-1} $KMnO_4$ was chosen for further studies, through a narrow linear range (12 - 24 mg COD L^{-1}) was achieved.

Table 22 Effect of $KMnO_4$ concentration on peak height and slope of standard KHP solutions (equivalent to COD concentration)

$KMnO_4$ (mmol L^{-1})	COD (mg L^{-1})	Peak height (mV)						Slope	r^2
		1	2	3	$\bar{X}$	Blank - $\bar{X}$	SD		
0.4	0 (blank)	1.45	1.48	1.47	1.47	0.00	0.02	4.70×10^{-2}	1
	12	0.62	0.60	0.64	0.62	0.85	0.02		
	24	0.07	0.07	0.07	0.07	1.40	0.00		
0.6	0 (blank)	2.64	2.61	2.62	2.62	0.00	0.02	5.52×10^{-2}	0.9912
	12	2.17	2.10	2.21	2.16	0.46	0.06		
	24	1.67	1.62	1.66	1.65	0.98	0.03		
	35	1.13	0.82	0.85	0.93	1.69	0.17		
0.8	0 (blank)	2.85	2.69	2.77	2.77	0.00	0.08	2.55×10^{-2}	0.9969
	12	2.44	2.44	2.40	2.42	0.35	0.02		
	24	2.03	2.08	2.07	2.06	0.71	0.03		
	35	1.64	1.92	1.78	1.78	0.99	0.14		
	59	1.22	1.22	1.18	1.21	1.56	0.02		

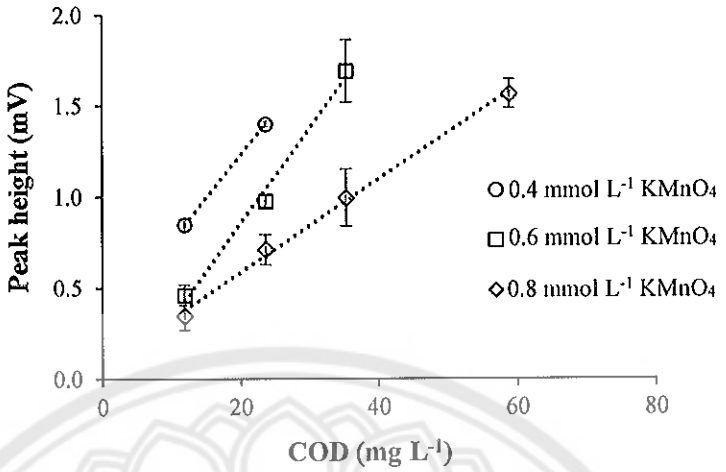

Figure 22 Effect of $KMnO_4$ concentration on peak height of standard KHP solutions (10 - 50 mg L^{-1} of KHP equivalent to 12 - 59 mg COD L^{-1})

2.3 Effect of H_2SO_4 concentration

The effect of H_2SO_4 concentrations (0.1-0.4 mol L^{-1}) was studied as it was a factor to accelerate oxidation reaction and to affect sensitivity and linearity of the calibration graph. Using obtained conditions in 2.2, blank and standard KHP solutions (5, 10 and 15 mg L^{-1} KHP equivalent to 6, 12 and 18 mg COD L^{-1}) were aspirated into the system. The results are shown in Table 23 and Figure 23. No different in slope of calibration graphs was found for all H_2SO_4 concentrations. Thus, a 0.2 mol L^{-1} H_2SO_4 was selected for further studies, as it provided a suitable of the sensitivity, linearity (r^2 = 0.9999) and chemicals economy.

Table 23 Effect of H_2SO_4 concentration on peak height and slope of standard KHP solutions (equivalent to COD concentration)

H_2SO_4 (mol L^{-1})	COD (mg L^{-1})	Peak height (mV)						Slope	r^2
		1	2	3	$\bar{X}$	Blank - $\bar{X}$	SD		
0.1	0 (blank)	1.77	1.75	2.08	1.87	0.00	0.19	7.17×10^{-2}	0.9984
	6	1.99	1.77	1.69	1.82	0.05	0.15		
	12	1.47	1.35	1.29	1.37	0.50	0.09		
	18	1.01	0.94	0.97	0.97	0.89	0.03		

Table 23 (cont.)

H_2SO_4 (mol L^{-1})	COD (mg L^{-1})	Peak height (mV)						Slope	r^2
		1	2	3	$\bar{X}$	Blank - $\bar{X}$	SD		
0.2	0 (blank)	1.79	1.76	1.63	1.73	0.00	0.08	7.46×10^{-2}	0.9999
	6	0.49	1.37	1.37	1.41	0.32	0.07		
	12	0.95	0.97	0.99	0.98	0.75	0.01		
	18	0.53	0.53	0.54	0.53	1.19	0.01		
0.3	0 (blank)	1.20	1.01	1.09	1.10	0.00	0.10	8.34×10^{-2}	0.9956
	6	1.08	1.05	1.10	1.08	0.02	0.02		
	12	0.61	0.53	0.46	0.53	0.57	0.07		
	18	0.11	0.08	0.10	0.10	1.00	0.01		
0.4	0 (blank)	0.90	1.04	1.23	1.06	0.00	0.17	7.81×10^{-2}	0.9052
	6	1.00	1.06	0.98	1.01	0.04	0.04		
	12	0.28	0.31	0.31	0.30	0.76	0.02		
	18	0.12	0.08	0.09	0.10	0.96	0.02		

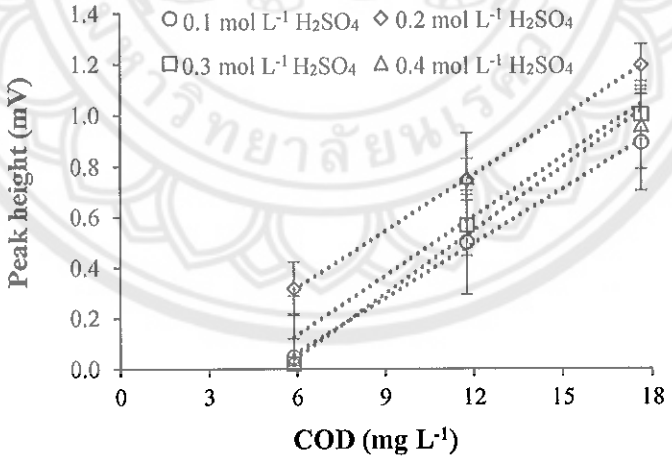

Figure 23 Effect of H_2SO_4 concentration on peak height of standard KHP solutions (5 - 15 mg L^{-1} of KHP equivalent to 6 - 18 mg COD L^{-1})

2.4 Effect of flow rate

In order to achieve good sensitivity, good digestion efficiency and rapid analysis time, the effect of flow rate of carrier was studied. Various flow rates

(0.8-1.4 mL min^{-1}) were varied and optimized. Using obtained conditions in 2.2 and 2.3, blank and standard KHP solutions (5, 10 and 15 mg L^{-1} KHP equivalent to 6, 12 and 18 mg COD L^{-1}) were aspirated into the system. The results are shown in Table 24 and Figure 24 and slopes were obtained. Flow rate of 0.8 mL min^{-1} resulted in the highest sensitivity (slope). This flow rate indicated good digestion efficiency, but it took long analysis time (8 min per injection). For flow rates of 1.2 (6:45 min per injection) and 1.4 mL min^{-1} (6:10 min per injection), sensitivity was decreased because of low digestion efficiency and low dispersion. Thus, the flow rate of 1.0 mL min^{-1} was selected as it provided a suitable slope, good linearity (r^2 = 0.9986) and rapid analysis time (7: 20 min per injection).

Table 24 Effect of flow rate on peak height and slope of standard KHP solutions (equivalent to COD concentration)

Flow rate (mL min^{-1})	COD (mg L^{-1})	Peak height (mV)						Slope	r^2
		1	2	3	$\bar{X}$	Blank - $\bar{X}$	SD		
0.8	0 (blank)	1.66	1.69	1.59	1.64	0.00	0.05	7.17×10^{-2}	0.9525
	6	1.39	1.24	1.34	1.32	0.32	0.08		
	12	0.84	0.75	0.80	0.80	0.85	0.04		
	18	0.62	0.53	0.53	0.50	1.08	0.05		
1.0	0 (blank)	1.62	1.67	1.70	1.66	0.00	0.04	7.46×10^{-2}	0.9986
	6	1.40	1.39	1.37	1.39	0.27	0.01		
	12	1.05	1.02	1.05	1.04	0.62	0.01		
	18	0.74	0.74	0.73	0.74	0.93	0.01		
1.2	0 (blank)	1.40	1.34	1.30	1.35	0.00	0.05	8.34×10^{-2}	0.9880
	6	1.14	1.17	1.20	1.17	0.15	0.03		
	12	0.80	0.82	0.78	0.80	0.52	0.02		
	18	0.54	0.53	0.51	0.53	0.82	0.01		
1.4	0 (blank)	1.39	1.46	1.36	1.40	0.00	0.05	7.81×10^{-2}	0.8865
	6	1.27	1.19	1.19	1.23	0.19	0.05		
	12	1.24	1.12	1.09	1.11	0.25	0.08		
	18	0.88	0.89	0.86	0.88	0.52	0.02		

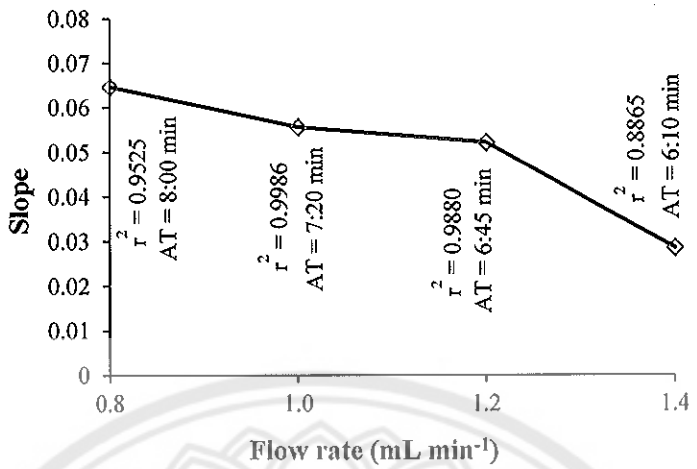

Figure 24 Effect of flow rate on slope of standard KHP solutions (5 - 15 mg L^{-1} KHP equivalent to 6 - 18 mg COD L^{-1}), when AT is analysis time.

2.5 Effect of reaction loop length at UV reactor

Reaction loop length is one of the important parameter in order to obtain high sensitivity, good dispersion efficiency and achieve a good digestion efficiency. The effect of reaction loop lengths (150-250 cm) were studied. Using the obtained conditions in 2.2-2.4, blank and standard KHP solutions (5, 10 and 15 mg L^{-1} KHP equivalent to 6, 12 and 18 mg COD L^{-1}) were aspirated into the system. Results in Table 25 and Figure 25 indicated that the reaction loop length of 200 cm gave the highest slope, good digestion efficiency, minimize peak broadening and acceptable analysis time (7:30 min per injection) for COD determination by the proposed system.

Table 25 Effect of reaction loop length at UV reactor on peak height and slope of standard KHP solutions (equivalent to COD concentration)

Reaction loop length (cm)	COD (mg L^{-1})	Peak height (mV)						Slope	r^2
		1	2	3	$\bar{X}$	Blank - $\bar{X}$	SD		
150	0 (blank)	1.51	1.50	1.50	1.50	0.00	0.00	1.89×10^{-2}	0.9374
	6	1.37	1.25	1.24	1.29	0.22	0.07		
	12	1.20	1.23	1.26	1.23	0.28	0.03		
	18	1.13	1.04	1.02	1.07	0.44	0.06		

Table 25 (cont.)

Reaction loop length (cm)	COD (mg L^{-1})	Peak height (mV)						Slope	r^2
		1	2	3	$\bar{X}$	Blank - $\bar{X}$	SD		
150	0 (blank)	1.51	1.50	1.50	1.50	0.00	0.00	1.89×10^{-2}	0.9374
	6	1.37	1.25	1.24	1.29	0.22	0.07		
	12	1.20	1.23	1.26	1.23	0.28	0.03		
	18	1.13	1.04	1.02	1.07	0.44	0.06		
200	0 (blank)	1.59	1.61	1.51	1.57	0.00	0.05	4.48×10^{-2}	0.9995
	6	1.35	1.30	1.25	1.30	0.27	0.05		
	12	1.05	1.03	1.06	1.07	0.50	0.01		
	18	0.87	0.72	0.73	0.77	0.80	0.09		
250	0 (blank)	1.71	1.63	1.50	1.61	0.00	0.10	4.34×10^{-2}	0.9965
	6	1.18	1.06	1.08	1.11	0.50	0.06		
	12	0.92	0.86	0.86	0.88	0.73	0.04		
	18	0.64	0.56	0.59	0.60	1.01	0.04		

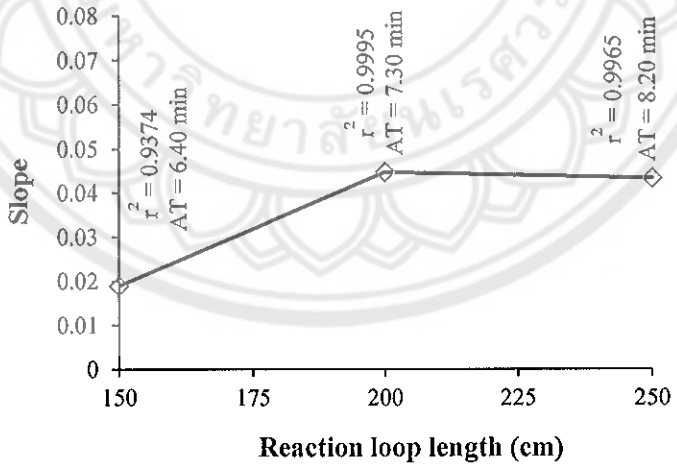

Figure 25 Effect of reaction loop length at UV reactor on slope of standard KHP solutions (5 - 15 mg L^{-1} of KHP equivalent to 6 - 18 mg COD L^{-1}), when AT is analysis time.

2.6 Effect of carrier solution using H_2SO_4

The effect of carrier solution using H_2SO_4 was studied in order to stabilize baseline and avoid manganese dioxide (MnO_2) precipitated in system. Various concentrations of H_2SO_4 (0, 0.1, 0.2 and 0.3 mol L^{-1}) were varied and optimized. Using the obtained conditions in 1.2 -2.5, blank and standard KHP solutions (5, 10 and 15 mg L^{-1} KHP equivalent to 6, 12 and 18 mg COD L^{-1}) were aspirated into the system. The results are shown in Table 26 and Figure 26. It could be seen that, at H_2SO_4 concentrations less than 0.2 mol L^{-1}, particulate manganese dioxide (MnO_2) were produced in the system while no MnO_2 was found at 0.2 and 0.3 mol L^{-1}. Therefore, a 0.2 mol L^{-1} H_2SO_4 of carrier stream was selected as providing highest sensitivity and less expense of chemical.

Table 26 Effect of carrier solution of H_2SO_4 on peak height and slope of standard KHP solutions (equivalent to COD concentration)

Carrier solution using H_2SO_4 (mol L^{-1})	COD (mg L^{-1})	Peak height (mV)						Slope	r^2
		1	2	3	$\bar{X}$	Blank - $\bar{X}$	SD		
0	0 (blank)	1.07	0.99	1.03	1.03	0.00	0.05	2.07×10^{-2}	0.9828
	6	0.78	0.75	0.77	0.77	0.26	0.01		
	12	0.62	0.68	0.72	0.67	0.36	0.05		
	18	0.60	0.49	0.48	0.52	0.51	0.06		
0.1	0 (blank)	1.52	1.52	1.48	1.51	0.00	0.02	4.73×10^{-2}	0.9997
	6	1.36	1.20	1.28	1.28	0.23	0.08		
	12	1.13	0.94	0.94	1.01	0.50	0.11		
	18	0.76	0.69	0.71	0.72	0.79	0.04		
0.2	0 (blank)	1.64	1.60	1.60	1.61	0.00	0.02	5.50×10^{-2}	0.9904
	6	1.46	1.39	1.32	1.39	0.22	0.07		
	12	1.06	1.01	0.96	1.01	0.60	0.05		
	18	0.77	0.75	0.71	0.74	0.87	0.03		

Table 26 (cont.)

Carrier solution using H_2SO_4 (mol L^{-1})	COD (mg L^{-1})	Peak height (mV)						Slope	r^2
		1	2	3	$\bar{X}$	Blank - $\bar{X}$	SD		
0.3	0 (blank)	1.65	1.62	1.61	1.63	0.00	0.02	5.50×10^{-2}	0.9981
	6	1.42	1.31	1.25	1.33	0.30	0.09		
	12	1.02	1.00	0.92	0.98	0.65	0.05		
	18	0.72	0.64	0.68	0.68	0.95	0.04		

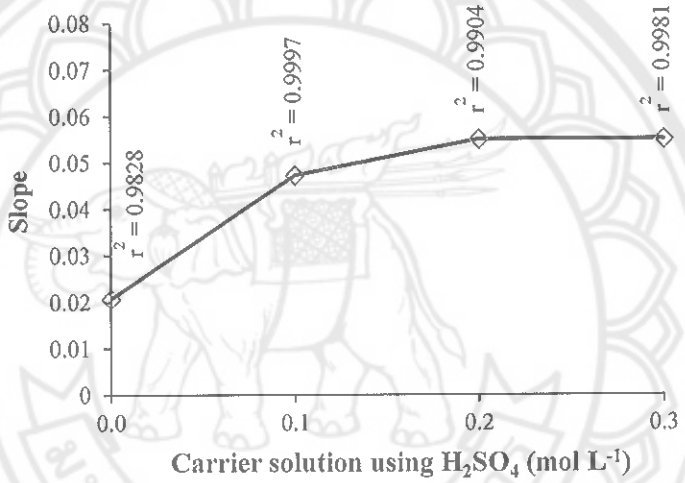

Figure 26 Effect of carrier solution using H_2SO_4 on slope of standard KHP solutions (5 – 15 mg L^{-1} of KHP equivalent to 6 - 18 mg COD L^{-1})

2.7 Effect of standard/sample and reagent volumes by mean of aspiration times

To maximize the sensitivity, good mixing of standard/sample and reagent and achieve an efficient oxidation reaction, the effect of standard/sample (V_S) and reagent (V_R) volumes was studied by mean of aspiration times in second using a homemade controller. Various V_S and V_R volumes (with aspiration time ratios (s:s) of 1:2, 2:3, and 3:4). Using obtained conditions in 2.1-2.6, blank and standard KHP solutions (5, 10 and 15 mg L^{-1} KHP equivalent to 6, 12 and 18 mg COD L^{-1}) were aspirated into the system. Results in Table 27 and Figure 27 indicated that the aspirated time of 2 seconds (15 µL) of standard/sample and 3 seconds (25 µL) of reagent should

be chosen as giving the highest slope (good sensitivity), good mixing of sample and reagent solution, good linearity ($r^2 = 0.9904$) and minimum peak broadening.

Table 27 Effect of standard/sample (Vs) and reagent (V_R) volumes by mean of aspiration times (in second) on peak height and slope of standard KHP solutions (equivalent to COD concentration)

$V_S : V_R$ (s:s)	COD (mg L^{-1})	Peak height (mV)						Slope	r^2
		1	2	3	$\bar{X}$	Blank - $\bar{X}$	SD		
1:2	0 (blank)	1.89	1.77	1.83	1.83	0.00	0.06	5.09×10^{-2}	0.9999
	6	1.65	1.53	1.47	1.55	0.28	0.09		
	12	1.31	1.18	1.27	1.25	0.58	0.07		
	18	1.01	0.91	0.94	0.95	0.88	0.05		
2:3	0 (blank)	1.64	1.60	1.60	1.61	0.00	0.02	5.50×10^{-2}	0.9904
	6	1.46	1.39	1.32	1.39	0.22	0.07		
	12	1.06	1.01	0.96	1.01	0.60	0.05		
	18	0.77	0.75	0.71	0.74	0.87	0.03		
3:4	0 (blank)	1.64	1.59	1.59	1.60	0.00	0.03	4.76×10^{-2}	0.9898
	6	1.33	1.26	1.24	1.28	0.33	0.05		
	12	1.06	0.89	0.90	0.65	0.66	0.10		
	18	0.73	0.72	0.70	0.72	0.89	0.01		

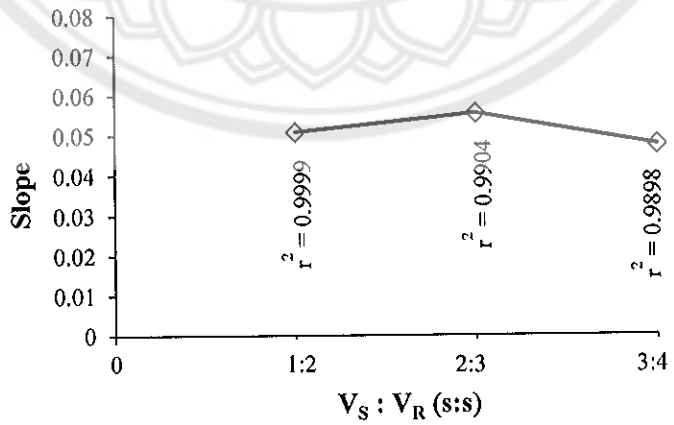

Figure 27 Effect of sample (Vs) and reagent (V_R) volumes by mean of aspiration time (in second) on slope of standard KHP solutions (5 - 15 mg L^{-1} KHP equivalent to 6 - 18 mg COD L^{-1})

2.8 Summary of condition used of the system using acidic $KMnO_4$ reagent solution

The rapid-SAFA spectrophotometric system with on-line UV photooxidation using acidified $KMnO_4$ based reaction is depicted in Figure 8 (c) and the optimum conditions are summarized in Table 28.

Table 28 Conditions used of the system for COD determination using acidic $KMnO_4$ reagent solution

Parameters	Conditions used
Rapid-SAFA system:	
Reagent solution	0.4 mmol L^{-1} $KMnO_4$ + 0.2 mol L^{-1} H_2SO_4
Carrier solution	0.2 mol L^{-1} H_2SO_4
UV reactor	36 W of UV lamp wound with PTFE tubing of 200 cm (i.d. 0.89 mm)
Flow rate	1.0 mL min^{-1}
Stopped time at UV reactor	0 s
Standard/sample and reagent volumes	15 µL and 25 µL (equal to 2 s and 3 s of aspiration times)
Detection wavelength	525 nm
Operation times of the system:	
1) Filling steps of;	
- carrier to UV reactor, FC and W_1	320 s
- reagent to W_2	20 s
- standard/sample to W_2	20 s
2) Loading step of;	
- rapid sequenced aspiration of standard/sample and reagent at L_{SR} to W_2	150 s
3) Injection step of;	
- standard/ sample plus reagent zone at UV reactor to FC and W_1	300 s
4) Cleaning steps of;	
- standard/sample to W_2	60 s
- reagent to W_2	60 s
- carrier to W_2	120 s

2.9 Analytical characteristic data of the system using acidic $KMnO_4$ reagent solution

Using the system as shown in Figure 8 (c) and the optimum conditions described in 2.8, blank and standard KHP solutions (3, 6, 10, 12 and 15 mg KHP L^{-1} equivalent to 4, 7, 11, 14 and 18 mg COD L^{-1}) were aspirated into the system. Under the optimum conditions, the results are shown in Table 29, Figure 28 (a) and (b). Linear range was obtained in the range of 4 - 18 mg COD L^{-1} (3 - 15 mg L^{-1} KHP) with linear equation of $y = 0.0536x - 0.1075$ ($r^2 = 0.9919$). The limit of detection (LOD) was 2.8 mg COD L^{-1} (2.3 mg L^{-1} KHP) expressing of $LOD = \bar{X} + 3SD_{blank}$. The relative standard deviation (RSD) was in the range of 1.1 – 5.3% and the sample throughput was 7.5 injections per hour.

Table 29 Calibration data of the system for COD determination using acidic $KMnO_4$ reagent solution

COD (mg L^{-1})	Peak height (mV)						
	1	2	3	$\bar{X}$	SD	%RSD	Blank - $\bar{X}$
0 (blank)	1.04	0.98	1.03	1.02	0.03	-	0.00
4	0.93	0.94	0.88	0.92	0.01	1.1	0.10
7	0.79	0.75	0.77	0.77	0.02	2.6	0.25
11	0.56	0.58	0.59	0.57	0.01	1.8	0.44
14	0.34	0.33	0.32	0.33	0.01	3.0	0.69
18	0.20	0.19	0.18	0.19	0.01	5.3	0.83

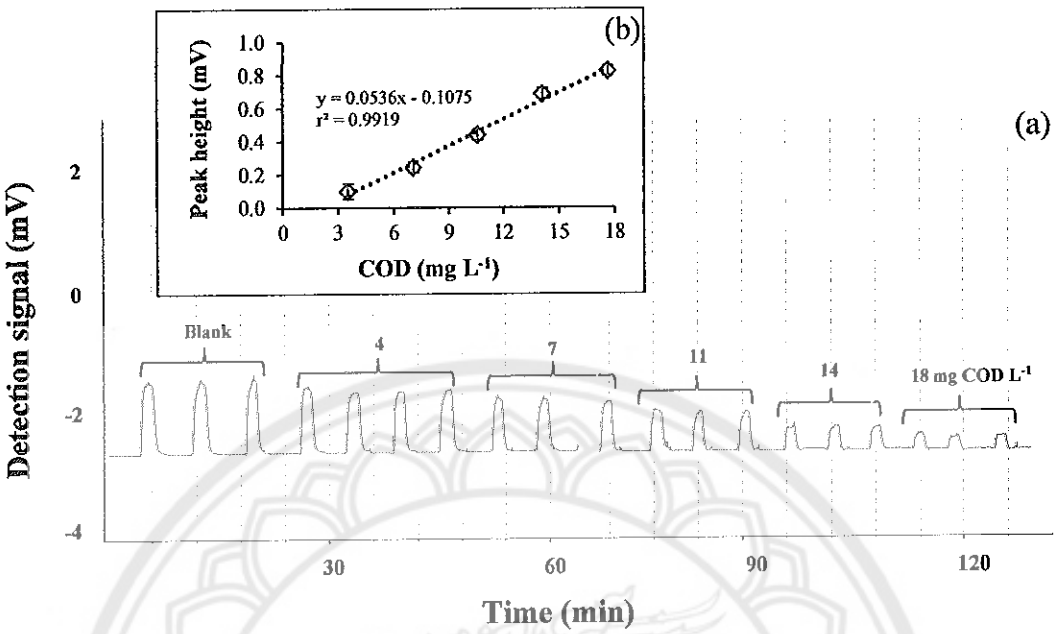

Figure 28 (a) Typical of a rapid-SAFA signals and (b) calibration graph for COD determination using acidic $KMnO_4$ reagent solution

3. Application of the rapid-SAFA system to real wastewater samples

The soluble COD contents in various sources of wastewater samples (i.e. agricultural drainage, domestic, hospital and pig farm) were determined by the rapid-SAFA spectrophotometry with on-line using both acidic $K_2Cr_2O_7$ and $KMnO_4$ reagent solutions. The results are shown in Table 30, Figure 29 (a) and Figure 29 (b), respectively. Results obtained in Table 30 of the proposed system were also validated with the standard titration method and by spiking standard KHP solutions (equivalent to 35 and 118 mg COD L^{-1}).

The COD values obtained from the proposed system using acidic $K_2Cr_2O_7$ reagent solution were in good agreement with those obtained from the proposed system using acidic $KMnO_4$ solution (t-test of $t_{calculation} = 0.34$ and $t_{critical} = 2.02$, 95% confidence level) and the standard titration method (t-test of $t_{calculation} = 0.17$, $t_{critical} = 2.02$, 95% confidence level). Meanwhile, the COD values obtained from the proposed system using acidic $KMnO_4$ were also in good agreement with those obtained from the standard titration method (t-test of $t_{calculation} = 0.40$, $t_{critical} = 2.02$, 95% confidence level). For the analysis of wastewater samples using acidified $K_2Cr_2O_7$ reagent solution, recoveries and

relative standard deviations by spiking two COD concentrations were obtained in the range of 74 - 131% and 0.3 - 10.3%, respectively. Meanwhile, the analysis of wastewater samples using acidified $KMnO_4$ reagent solution, recoveries and relative standard deviations from spiking two COD concentrations were obtained in the range of 70 - 128 and 0.2 - 7.9%, respectively. Moreover, the proposed system using both acidified $K_2Cr_2O_7$ and $KMnO_4$ based reaction were also evaluated by correlation coefficient graph. The correlation graphs are shown in Figure 30 (a), (b) and (c). It was concluded that good agreement between the proposed systems and the standard titration method were found with correlation coefficient of $r^2 = 0.9804$ (see in Figure 30 (a)) and $r^2 = 0.9877$ (see in Figure 30 (b)), respectively. And good correlation coefficient between the proposed systems using $K_2Cr_2O_7$ and $KMnO_4$ was obtained $r^2 = 0.9596$ (see in Figure 30 (c)).

Table 30 Soluble COD contents (mg L^{-1}) in wastewater sample, as determined by the proposed rapid-SAFA spectrophotometric system using acidified $K_2Cr_2O_7$ and $KMnO_4$ based reaction and the standard titration method

Waste water	No.	Added (mg COD L^{-1})	Concentration found (mg COD L^{-1}) ; n=3								
			Rapid-SAFA system using acidic $K_2Cr_2O_7$			Rapid-SAFA system using acidic $KMnO_4$			Standard titration method		
			$\bar{X}$±SD*	%RSD**	%Rec***	$\bar{X}$±SD	%RSD	%Rec	$\bar{X}$±SD	%RSD	%Rec
Agricultural drainage 1	1	-	41±4 (103±10) ****	9.8	-	37±2 (93±5)	5.4	-	43±4 (108±10)	9.3	-
	2	35	70±3	4.3	83±9	69±0.5	0.7	91±2	76±4	5.3	94±12
	3	118	146±8	5.5	89±7	160±1	0.6	104±1	148±5	3.4	89±4
Agricultural drainage 2	4	-	ND*****	-	-	9±0.3 (23±0.8)	3.3	-	16±2 (40±5)	12.5	-
	5	35	39±3	7.7	111±9	51±1	2.0	120±3	46±2	4.3	86±6
	6	118	148±8	5.4	125±7	108±3	2.8	84±3	133±2	1.5	99±2
Agricultural drainage 3	7	-	265±1 (663±3)	0.4	-	268±8 (670±20)	3.0	-	254±8 (635±20)	3.1	-
	8	35	306±3	1.0	117±9	295±3	1.7	77±9	284±2	0.7	86±6
	9	118	374±6	1.6	92±5	365±7	1.6	82±5	362±6	1.7	92±6
Domestic 1	10	-	43±6 (108±15)	14.0	-	41±2 (103±5)	4.9	-	36±3 (90±8)	8.3	-
	11	35	80±3	3.8	106±9	72±2	2.8	89±6	72±5	6.9	103±14
	12	118	141±6	4.3	83±5	163±3	1.8	103±3	152±4	2.6	98±4
Domestic 2	13	-	47±3 (118±8)	6.4	-	45±3 (113±8)	6.7	-	51±7 (128±18)	13.7	-
	14	35	83±3	3.6	103±9	73±1	1.4	80±3	82±6	7.3	89±18
	15	118	166±3	1.8	101±3	165±1	0.6	102±1	166±3	1.8	97±3

Table 30 (cont.)

Waste water	No.	Added (mg COD L^{-1})	Concentration found (mg COD L^{-1}) ; n=3								
			Rapid-SAFA system using acidic $K_2Cr_2O_7$			Rapid-SAFA system using acidic $KMnO_4$			Standard titration method		
			$\bar{X}$±SD*	%RSD**	%Rec***	$\bar{X}$±SD	%RSD	%Rec	$\bar{X}$±SD	%RSD	%Rec
Domestic 3	16	-	36±3 (90±8)	8.3	-	49±1 (123±3)	2.0	-	42±6 (105±15)	14.3	-
	17	35	75±3	4.0	111±9	84±4	4.8	100±11	68±3	4.4	74±9
	18	118	153±5	3.3	99±4	155±2	1.3	90±2	153±1	0.7	94±1
Domestic 4	19	-	294±3 (735±8)	1.0	-	286±2 (715±5)	0.7	-	276±4 (690±10)	1.4	-
	20	35	327±3	0.9	94±9	311±4	1.3	71±11	315±2	0.6	111±6
	21	118	420±5	1.2	107±4	378±2	0.5	78±3	383±5	1.3	91±5
Domestic 5	22	-	276±1 (690±3)	0.4	-	283±2 (708±5)	0.7	-	275±3 (688±8)	1.1	-
	23	35	306±1	0.3	86±3	311±4	1.3	80±11	311±6	1.9	103±17
	24	118	411±6	1.5	114±5	366±3	0.8	70±3	374±4	1.1	84±3
Domestic 6	25	-	ND	-	-	8±1 (20±3)	13.0	-	9±1 (23±3)	11.1	-
	26	35	29±3	10.3	83±9	49±2	4.1	117±6	50±6	12.0	117±17
	27	118	90±8	8.9	76±7	153±5	3.3	123±4	130±4	3.1	103±4
Domestic 7	28	-	29±3 (73±8)	10.3	-	25±0.3 (63±0.8)	1.2	-	41±2 (103±5)	4.8	-
	29	35	75±3	4.0	131±9	62±4	6.5	106±11	80±3	3.8	111±9
	30	118	154±4	2.6	106±3	172±2	1.2	125±2	157±8	5.1	98±7
Domestic 8	31	-	68±6 (170±15)	8.8	-	81±0.4 (203±1)	0.5	-	76±7 (190±18)	9.2	-
	32	35	94±3	3.2	74±9	116±3	2.6	100±9	118±8	6.8	120±23
	33	118	193±9	4.7	106±8	221±1	0.5	119±1	201±7	3.5	106±6

Table 30 (cont.)

Waste water	No.	Added (mg COD L^{-1})	Concentration found (mg COD L^{-1}) ; n=3								
			Rapid-SAFA system using acidic $K_2Cr_2O_7$			Rapid-SAFA system using acidic $K_2Cr_2O_7$			Rapid-SAFA system using acidic $K_2Cr_2O_7$		
			$\bar{X}$±SD*	%RSD**	%Rec***	$\bar{X}$±SD	%RSD	%Rec	$\bar{X}$±SD	%RSD	%Rec
Domestic 9	34	-	34±1 (85±3)	2.9	-	26±2 (65±5)	7.7	-	29±4 (73±10)	14.0	-
	35	35	66±3	4.5	91±9	60±3	5.0	97±9	61±3	4.9	91±9
	36	118	165±7	4.2	111±6	127±10	7.9	86±8	135±2	1.5	90±2
Hospital 1	37	-	ND (< LOD)*****	-	-	10±0.3 (25±0.8)	3.0	-	14±2 (35±5)	14.3	-
	38	35	33±3	9.1	94±9	54±1	1.9	126±3	53±1	1.9	111±3
	39	118	97±3	3.1	82±3	142±5	3.5	112±4	134±2	1.5	102±1
Hospital 2	40	-	ND (< LOD)	-	-	16±1 (40±3)	6.3	-	28±2 (70±5)	7.1	-
	41	35	43±2	4.7	123±6	60±3	5.0	126±9	65±2	3.1	106±6
	42	118	106±2	1.9	90±2	167±0.4	0.2	128±0.3	135±5	3.7	91±5
pig farm	43	-	83±8 (208±20)	9.6	-	76±8 (190±20)	10.5	-	74±2 (185±5)	2.7	-
	44	35	118±1	0.8	100±3	115±1	0.9	111±3	110±2	1.8	103±6
	45	118	179±7	3.9	81±6	159±9	5.7	70±8	193±1	0.5	101±1

* Average value ± standard deviation of triplicate results ($\bar{X}$±SD); n=3

** %Relative standard deviation = (SD ÷ $\bar{X}$) × 100

*** %Recovery = [(concentration added – concentration found) ÷ concentration added)] × 100

**** COD concentrations were found by comparing the calibration graph of each sample (actual COD values in sample were calculated by considering dilution factor of each sample)

***** ND - Not detected (or less than LOD)

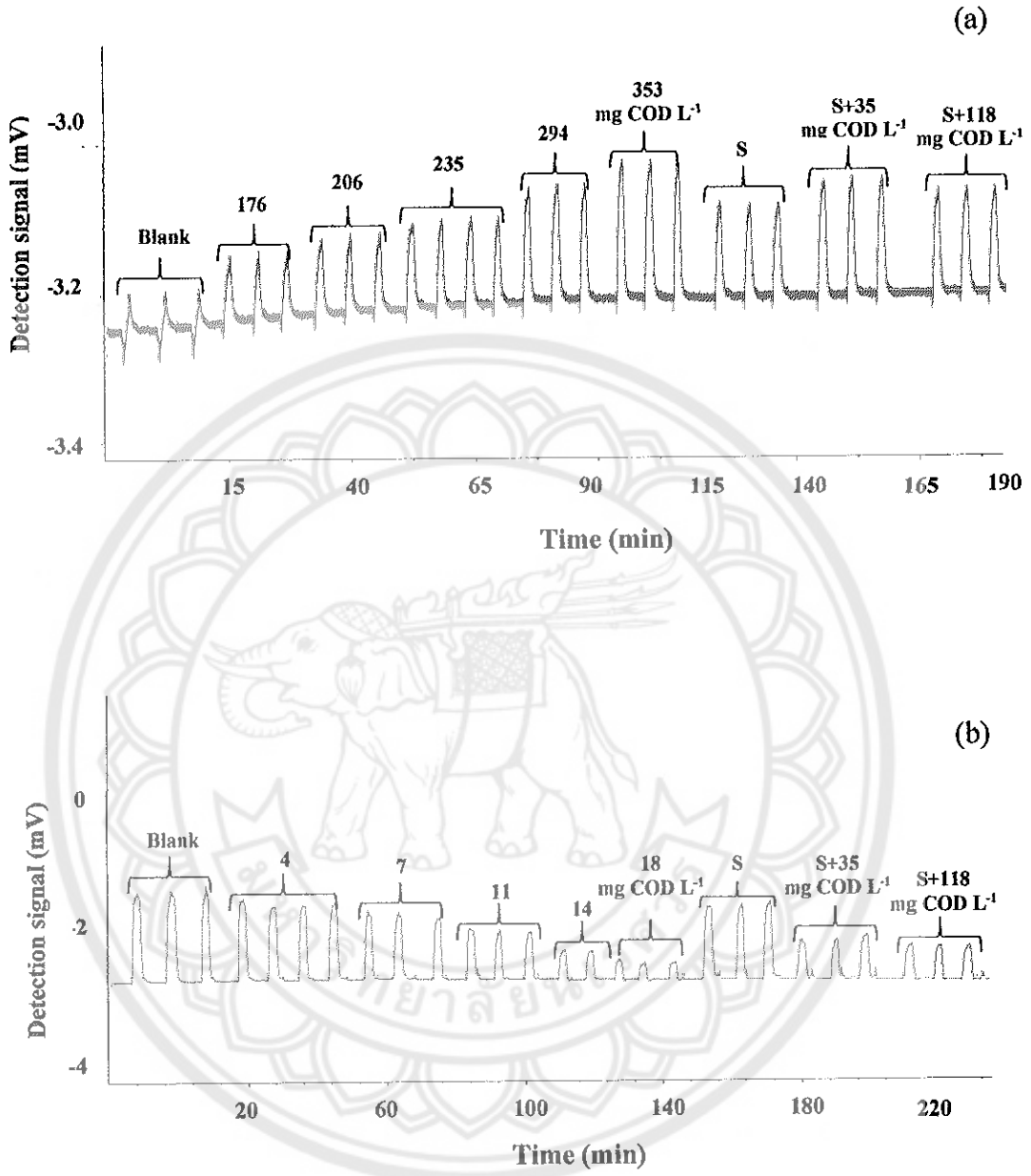

Figure 29 Typical of a rapid-SAFA signals for COD determination using: (a) acidic $K_2Cr_2O_7$ and (b) acidic $KMnO_4$ reagent solutions

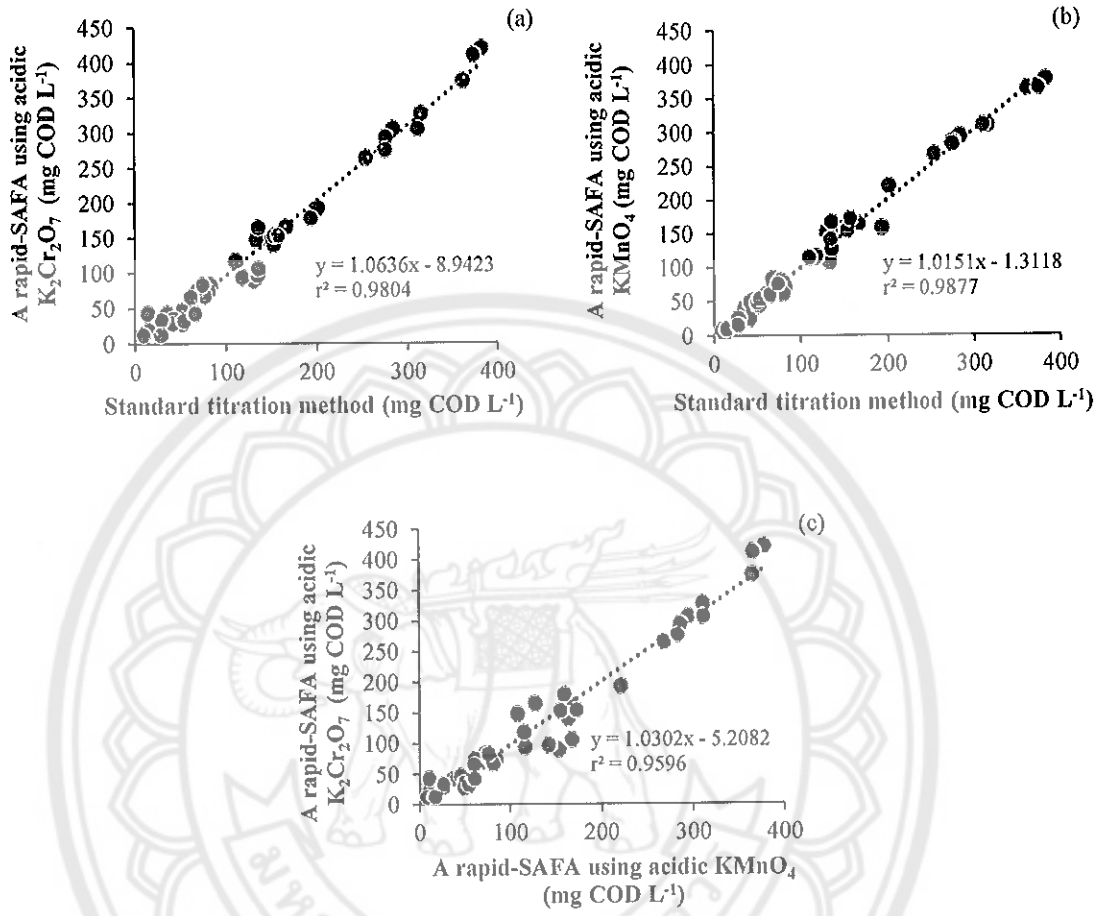

Figure 30 Correlation plots between the COD contents of real wastewater samples by: (a) a rapid-SAFA using acidic $K_2Cr_2O_7$ reagent solution and the standard titration method, (b) a rapid-SAFA using acidic $KMnO_4$ reagent solution and the standard titration method and (c) a rapid-SAFA using acidic $K_2Cr_2O_7$ reagent solution and a rapid-SAFA using acidic $KMnO_4$ reagent solution

REFERENCES

REFERENCES

[1] Chin, A. D. (2006). **Water-quality engineering in natural system.** New Jersey: John Wiley & Sons.

[2] Punmia, B.C. and Jain, A. K. (1998). **Wastewater engineering.** Boston: Sudha Offset Press.

[3] Drinan, J. E. and Spellman, F. R. (2013). **Water and wastewater treatment** (2nd ed.). London: CRC Press

[4] Clescer, L. S., Greenbery, A. E. and Eaton, A. D. (1998). **Standard methods for the examination of water and wastewater** (20th ed.). New York: American Public Health Association.

[5] Domini, C. E., Hidalgo, M., Marken, F. and Canals, A. (2006). Comparison of three optimized digestion methods for rapid determination of chemical oxygen demand: Closed microwaves, open microwaves and ultrasound irradiation. **Analytica Chimica Acta**, 561, 210-217.

[6] Yadvika, Yadav, A. K., Sreekrishnan, T. R., Satya, S. and Kohli, S. (2006). A modified method for eatimation of chemical oxygen demand for samples having high suspended solids. **Bioresource Technology**, 97, 721-726.

[7] Canals, A., Cuesta, A., Gras, L. and Hernandez, M. R. (2002). New ultrasound assisted chemical oxygen demand determination. **Ultrasonics Sonochemistry**, 9, 143-149.

[8] Ramon, R., Valero, F. and Valle, M. D. (2003). Rapid determination of chemical oxygen demand using a focused microwave heating system featuring temperature control. **Analytica Chimica Acta**, 491, 99-109.

[9] Raposo, F., de la Rubia, M. A. Borja, R. and Alaiz, M. (2008). Assessment of a modified and optimized method for determining chemical oxygen demand of solid substrates and solutions with high suspended solid content. **Talanta**, 76, 448-453.

[10] Li, J., Tao, T., Li, X., Zuo, J., Li, T., Lu, J., et al. (2009). A spectrophotometric method for determination of chemical oxygen demand using home-made reagent. **Desalination**, 239, 139-145.

[11] Domini, C. E., Vidal, L. and Canals, A. (2009). Trivalent manganese as an environmentally friendly oxidizing reagent for microwave and ultrasound-assisted chemical oxygen demand determination. **Ultrasonics Sonochemistry**, 16, 686-691.

[12] Chai, Y., Ding, H., Zhang, Z., Xian, Y., Pan, Z. and Jin, L. (2006). Study on photocatalytic oxidation for determination of the low chemical oxygen demand using a nano-TiO_2-$Ce(SO_4)_2$ coexisted system. **Talanta**, 68, 610-615.

[13] Hu, Y. and Yang, Z. (2004). A simple chemiluminescence method for determination of chemical oxygen demand values in water. **Talanta**, 63, 521-526.

[14] Yao, H., Wu, B., Qu, H. and Cheng, Y. (2009). A high throughput chemiluminescence method for determination of chemical oxygen demand in waters. **Analytica Chimica Acta**, 633, 76-80.

[15] Li, C. and Song, G. (2009). Photocatalytic degradation of organic pollutants and detection of chemical oxygen demand by fluorescence method. **Sensors and Actuator B**, 137, 432-436.

[16] Wang, J., Li, K., Yang, C., Wang, Y. and Jia, J. (2012). Ultrasound electrochemical determination of chemical oxygen demand using boron-doped diamond electrode. **Electrochemistry Communications**, 18, 51-54.

[17] Dan, D., Dou, F., Xiu, D. and Qin, Y. (2000). Chemical oxygen demand determination in environmental waters by mixed-acid digestion and single sweep polarography. **Analytica Chimica Acta**, 420, 39-44.

[18] Ma, C., Tan, F., Zhao, H., Chen, S. and Quan, X. (2011). Sensitive amperometric determination of chemical oxygen demand using Ti/Sb-SnO_2/PbO_2 composite electrode. **Sensors and Actuators B**, 155, 114-119.

[19] Tian, C. L. and Wu, M. S. (1992). Determination of chemical oxygen demand in aqueous environmental samples by segmented flow injection analysis. **Analytica Chimica Acta**, 216, 301-305.

[20] Balconi, M. L., Borgarello, M., Ferraroli, R. and Realini, F. (1992). Chemical oxygen demand determination in well and river waters by flow injection analysis using a microwave oven during the oxidation step. **Analytica Chimica Acta**, 216, 295-299.

[21] Cuesta, A., Todoli, L. J. and Canals, A. (1996). Flow injection method for the rapid determination of chemical oxygen demand based on microwave digestion and chromium speciation in flame absorption spectrometry. **Spectrochimica Acta part B**, 51, 1791-1800.

[22] Pecharroman, B. V., Reina, A. L. and Luque de Castro, M. D. (1999). Flow injection determination of chemical oxygen demand in leaching liquid. **Analyst**, 124, 1261-1264.

[23] Li, B., Zhang, Z., Wang, J. and Xu, C. (2003). Chemiluminescence system for automatic determination of chemical oxygen demand using flow injection analysis. **Talanta**, 61, 651-658.

[24] Li, J., Li, L., Zheng, L., Xian, Y., Ai, S. and Jin, L. (2005). Amperometric determination of chemical oxygen demand with flow injection analysis using F-PbO_2 modified electrode. **Analytica Chimica Acta**, 548, 199-204.

[25] Dan, D., Sanford, R. C. and Worsfold, P. J. (2005). Determination of chemical oxygen demand in fresh waters using flow injection with on-line UV-photocatalytic oxidation and spectrophotometric detection. **Analyst**, 130, 227-232.

[26] Zenki, M., Fujiwara, S. and Yokoyama, T. (2006). Repetitive determination of chemical oxygen demand by cyclic flow injection analysis using on-line regeneration of consumed permanganate. **Analytical Science**, 22, 77-80.

[27] Su, Y., Li, X., Chen, H., Lv, Y. and Hou, X. (2007). Rapid, sensitive and on-line measurement of chemical; oxygen demand by novel optical method based on UV photolysis and chemiluminescence. **Microchemical Journal**, 87, 56-61.

[28] Jinjun, T., Yonggang, H. and Jie, Z. (2008). Chemiluminescence detection of permanganate index (COD_{Mn}) by a luminol-KMnO4 based reaction. **Journal of Environmental Sciences**, 20, 252-256.

[29] Almeida, C. A., Gonzalez, P., Mallea, M., Martinez, L. D and Gil, R. A. (2012). Determination of chemical oxygen demand by a flow injection method based on microwave digestion and chromium speciation coupled to inductively coupled plasma optical emission spectrometry. **Talanta,** 97, 273-278.

[30] Almeida, C. A., Savio, M., Gonzalez, P., Martinez, L. D and Gil, R. A. (2013). Determination of chemical oxygen demand employed manganese as an environmentally friendly oxidizing reagent by a flow injection method based on microwave digestion and speciation coupled to ICP-OES. **Microchemical Journal**, 106, 351-356.

[31] Mesquita, R. B. R. and Rangel, A. O. S. S. (2009). A review on sequential injection method for water analysis. **Analytica Chimica Acta**, 648, 7-22.

[32] Barnett, N. W., lenehan, C. E. and Lewis, S. W. (1999). Sequential injection analysis: an alternative approach to process analytical chemistry. **Trends in analytical chemistry**, 18, 346-353.

[33] Tue-Ngen, O., Eillis, P., McKelvie, I. D., Sandford, R. C., Worsfold, P. J., Jakmunee, J., et al. (2005). Determination of dissolved reactive phosphorus (DRP) and dissolved organic phosphorus (DOP) in natural waters by the use of rapid sequenced reagent injection flow analysis. **Talanta**, 66, 453-460.

[34] Tue-Ngen, O., Sandford, R. C., Jakmunee, J., Grudpan, K., McKelvie, I. D. and Worsfold, P. J. (2005). Determination of dissolved inorganic carbon (DIC) and dissolved organic carbon (DOC) in freshwater by sequential injectiob spectrophotometry with on-line UV photooxidation. **Analytica Chimica Acta,** 554, 17-54.

[35] Pons, C., Dorteza, R., Rangel, A. O. S. S. and Cerda, V. (2006). The application of multimmutated flow techniques to the determination of ion. **Trend in Analytical Chemistry,** 25, 583-588.

[36] Cerda, V., Forteza, R. and Estela, J. M. (2007). Potential of multisyringe flow-based multicommutated systems. **Analytica Chimica Acta,** 600, 35-45.

[37] Riffat, R. (2013). **Fundamentals of wastewater treatment and engineering.** London: CRC Press.

[38] Chapman, D. (1996). **Water quality assessments** (2nded.). London: Chapman & Hall.

[39] Gray, N. F. (1999). **Water technology an introduction for scientists and engineers**. Great Britain: Arnold

[40] Ibanez, J. G., Hernandez-Esparza, M., Doria-Serrano, C., Fregoso-Infante, A. and Singh, M. M. (2007). **Environmental chemistry fundamentals.** New York: Springer Science+Business Media.

[41] Yen, T. F. (2005). **Environmental chemistry: Chemistry of major environmental cycles**. London: Imperial College press.

[42] Pollution Control Department (PCD) Ministry of Natural Resource and Environment. (2004). **Water quality standards**. Retrieved February 1, 2014, from http://www.pcd.go.th/info_serv/en_reg_std_water01.html

[43] Ruzicka, J. (2015). **Flow injection analysis**. Retrieved February 5, 2015, from http://www.flowinjectiontutorial.com.

[44] Maya, F., Estela, J. M. and Cerda, V. (2010). Flow analysis techniques as effective tools for the improved environmental analysis of organic compounds expressed as total indices. **Talanta**, 81, 1-8.

[45] Ruzicka, J. and Hansen, E. H. (1988). **Flow injection analysis** (2nd ed.). New York: John Wiley & Sons.

[46] **Flow Injection Analysis**. Retrieved February 5, 2014, from http://www.diss.fuberlin.de/diss/servlets/MCRFileNodeServlet/FUDISS_derivate_000000001584/03_Kapitel02.pdf.?hosts.

[47] Ashish, P., Kamlesh, P., Chetan, P. and Patel, B. (2010). Flow injection: A new approach in analysis. **Chemical and Pharmaceutical Research**, 2(2), 118-125.

[48] Trojanowicz, M. (2000). **Flow injection analysis instrumentation and applications.** Singapore: Regal press.

[49] **Introduction to flow injection analysis (FIA)**. Retrieved January 6, 2015, from http://ww2.chemistry.gatech.edu/class/analyt/fia.pdf.

[50] Hansen, E. H., and Miró, M. (2009). **Flow injection analysis in industrial biotechnology**. Retrieved January 16, 2015, from http://onlinelibrary.wiley.com/

[51] Kolev, S. D. and Mckelvie, I. D. (2008). **Advances in flow injection analysis and related techniques.** New Jersey: John Wiley & Sons.

[52] Global FIA for Zone Fluidics instruments and components. (2008). **FIA/SIA tutorial.** Retrieved March 29, 2015, from http://www.globalfia.com.

[53] Skoog, A., West, M., Holler, F. and Crouch, R. (2004). **Fundamentals of analytical chemistry**. California: Thomson Brooks/Cole.

[54] Valcarcel, M. and Luque de Castro, M. D. (1988). **Automatic method of analysis.** Netherlands: Physical Science & Engineering Divition.

[55] Van Staden, J. F and Stefan, R. I. (2004). Chemical speciation by sequential injection analysis: an overview. **Talanta**, 64, 1109-1113.

[56] Cerda, V. and Pons, C. (2006). Multicommutated flow techniques for developing analytical methods. **Analytical Chemistry**, 25, 236-242.

[57] Sixto, A. and Knochen, M. (2009). Multicommutated flow system for the determination of glucose in honey with immobilized glucose oxidase reactor and spectrophotometric detection. **Talanta**, 77, 1534-1538.

APPENDIX

APPENDIX A THE IMAGE OF A HOMEMADE RAPID-SAFA SPECTRO-PHOTOMETRIC SYSTEM AND A STANDARD TITRATION METHOD UESD IN THIS RESEARCH

A.1 The image of a homemade rapid-SAFA spectrophotometric system with on-line UV photooxidation for COD determination of wastewater

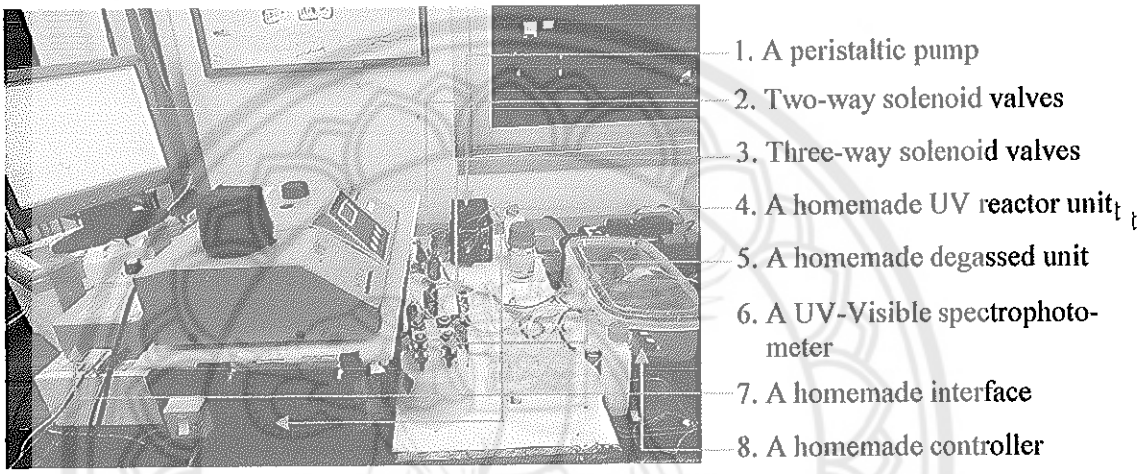

Figure 31 Setup of a homemade rapid-SAFA spectrophotometric system, designed and constructed by Chanyud Kritsunankul, Orawan Kritsunankul and Jaroon Jakmunee

A.2 The image and procedure of a standard titration method COD determination of water and wastewater

The apparatuses used in the standard method are shown in Figure 32. The test procedure was to add 2.5 mL of a known quantity of standard/sample, 1.5 mL of 0.0167 mol L^{-1} $K_2Cr_2O_7$, and 3.5 mL of concentrated H_2SO_4 solution into a digestion tube. This mixing solution was refluxed for 2 hours at 150°C using a controlled-temperature oven. After digestion, it was cooled before titration. The remaining $K_2Cr_2O_7$ was then titrated with 0.1 mol L^{-1} of ferrous ammonium sulfate standard solution using ferroin as indicator. With an end point color change from blue-green to reddish-brown. A blank solution of ultrapure water is carried out through the same procedure as the wastewater sample.

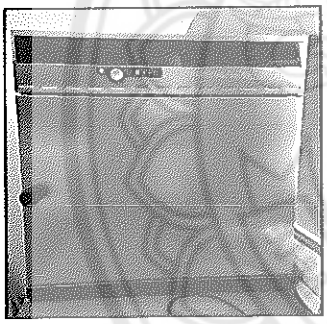

A controlled-temperature oven

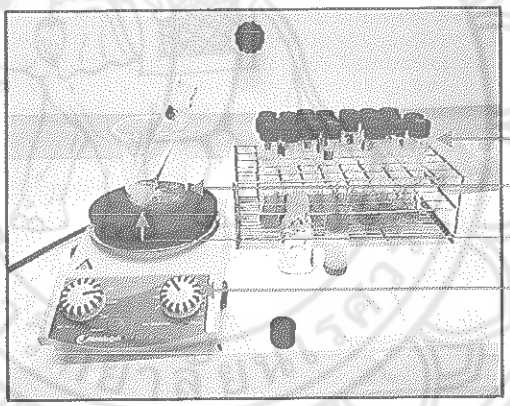

Figure 32 Setup of a standard titration method

APPENDIX B CALCULATION OF A THEORETICAL COD VALUE FROM POTASSIUM HYDROGEN PHTHALATE STANDARD SOLUTION

Generally, the COD content in water and wastewater is depended on the COD mass equivalent to organic compound used as a standard solution of each COD test. Thus, in this work, the calculation of a theoretical of COD value from a potassium hydrogen phthalate (KHP) was carried out. This value could be calculated by two redox stoichiometry reactions as follows.

B.1 Calculation of the theoretical COD value from the redox reaction of KHP and oxygen

The stoichiometry of redox reaction of KHP and oxygen is shown in equation (1):

$$\underset{\text{(KHP)}}{2KC_8H_5O_4\,(aq)} + 15O_2\,(g) \longrightarrow K_2O\,(aq) + 16CO_2\,(g) + 5H_2O\,(l) \quad .....(1)$$

A redox stoichiometry indicates that the oxidation of KHP (MW = 204.23 g mol^{-1}) is accomplished through reduction of oxygen (MW = 32 g mol^{-1}) to carbon dioxide (CO_2) and water (H_2O) and described as following;

When, 2 mol of KHP = 15 mol of O_2

$$2 \text{ mol} \times 204.23 \text{ g mol}^{-1} \text{ of KHP} = 15 \text{ mol} \times 32 \text{ g mol}^{-1} \text{ of } O_2$$

Thus,
$$1 \text{ g of KHP} = \frac{15 \text{ mol} \times 32 \text{ g mol}^{-1} \text{ of } O_2}{2 \text{ mol} \times 204.23 \text{ g mol}^{-1}}$$
$$= 1.176 \text{ g } O_2$$

It could be concluded that a 1 g of KHP is equivalent to 1.176 g O_2. Hence, a 1000 mg L^{-1} KHP has a theoretical COD value of 1176 mg L^{-1} (1 g KHP L^{-1} = 1.176 g COD L^{-1}).

B.2 Calculation of the theoretical COD value from the redox reaction of KHP and acidic potassium dichromate

The stoichiometry of redox reaction of KHP and acidic potassium dichromate ($K_2Cr_2O_7$) is shown in equation (2):

$$2KC_8H_5O_4(aq) + 10K_2Cr_2O_7(aq) + 41H_2SO_4(aq) \xrightarrow{\text{(KHP)}} 10Cr_2(SO_4)_3(aq) + 16CO_2(g) + 46H_2O(l) + 11K_2SO_4(aq) \quad .....(2)$$

A redox stoichiometry indicates that the oxidation of KHP (MW = 204.23 g mol^{-1}) is accomplished through reduction of $K_2Cr_2O_7$ (MW = 294.23 g mol^{-1}) to chromic (Cr^{3+}) ion, carbon dioxide (CO_2) and water (H_2O) and described as following;

When, 2 mol of KHP = 10 mol of $K_2Cr_2O_7$

2 mol × 204.23 g mol^{-1} of KHP = 10 mol × 294.18 g mol^{-1} of $K_2Cr_2O_7$

Thus, 1 g of KHP = $\dfrac{10 \text{ mol} \times 294.18 \text{ g mol}^{-1} \text{ of } K_2Cr_2O_7}{2 \text{ mol} \times 204.23 \text{ g mol}^{-1}}$

= 7.2067 g of $K_2Cr_2O_7$

It could be seen that a 1 g of KHP is equivalent to a 7.2067 g of $K_2Cr_2O_7$. For the calculation of $K_2Cr_2O_7$ mass equivalent to O_2 mass, the equation (3) and (4) is used to calculate as described below.

$$Cr_2O_7^{2-}(aq) + 14H^+(aq) + 6e^- \rightarrow Cr^{3+}(aq) + 7H_2O(l) \quad .....(3)$$

$$O_2(g) + 4e^- \rightarrow 2e^{2-} \quad .....(4)$$

Then,

$$\frac{\text{mol } e^- \text{ } Cr_2O_7^{2-}}{\text{mol } e^- \text{ } O_2} = \frac{6}{4}$$

$$\text{mol } e^- \text{ } Cr_2O_7^{2-} = \frac{6}{4} \text{ mol } e^- \text{ } O_2$$

$$= 1.5 \times \text{mol } O_2$$

$$= 1.5 \times 32 \text{ g } O_2$$

Thus, 1 mol × 294.18 g mol^{-1} of $Cr_2O_7^{2-}$ = 48 g O_2

From, the calculation as described above, 1 g of KHP is equivalent to a 7.2067 g of $K_2Cr_2O_7$.

Thus, 294.18 g of $K_2Cr_2O_7$ = 48 g O_2

$$7.2067 \text{ g of } K_2Cr_2O_7 = \frac{48 \text{ g} \times 7.2067 \text{ g}}{294.18 \text{ g}} = 1.176 \text{ g } O_2$$

It could be concluded that a 1 g of KHP is equivalent to 1.176 g O_2. Hence, a 1000 mg L^{-1} KHP is equal to a theoretical COD value of 1176 mg L^{-1} (1 g KHP L^{-1} = 1.176 g COD L^{-1}).